Chemical Engineering & Processing: Process Intensification 208 (2025) 110078

Contents lists available at ScienceDirect

Chemical Engineering and Processing - Process Intensification

journal homepage: www.elsevier.com/locate/cep

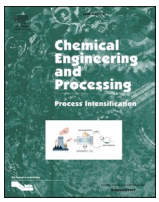

A process intensification 4.0 approach to determine the feasibility and sustainability of producing biojet-fuel by alcohol to jet route. A case of study of Mexico

David Vallejo-Blancas [a], Eduardo Sánchez-Ramirez [a], José María Ponce-Ortega [b], Juan Gabriel Segovia-Hernández [a], Juan José Quiroz Ramírez [c], Gabriel Contreras-Zarazúa [d,*]

[a] Department of Chemical Engineering University of Guanajuato, Noria Alta S/N,36000, Guanajuato,Gto., Mexico
[b] Chemical Engineering Department, Universidad Michoacana de San Nicolás de Hidalgo, Morelia, Michoacán 58060, Mexico
[c] CONACyT- CIATEC, Center for Applied Innovation in Competitive Technologies
[d] Chemical Engineering Area, Department of Process and Hydraulic Engineering, Metropolitan Autonomous University-Iztapalapa, Av. FFCC R. Atlixco 186, 09340 Iztapalapa, Mexico City, Mexico

ARTICLE INFO

Keywords:
Development goals
Supply chain
Modular processing
CO2 reduction
ATJ process

ABSTRACT

This paper explores the feasibility of producing biojet-fuel in Mexico using the Alcohol to Jet process as the base production technology. The work develops a mathematical model based on a process intensification 4.0 approach, which considers the modularization and decentralization of different parts of the process across various locations, with the aim of improving the sustainability of the process. Corn stover and sugarcane bagasse were considered as feedstocks. The mathematical model was formulated as a mixed-integer linear programming problem and solved through multi-objective optimization, focusing on maximizing net profit and social welfare while minimizing the environmental impact as measured by the Eco-indicator 99. This metrics evaluates economics, environmental and social issues. In addition, the generation of jobs calculated using the Jobs Economic Development Impact models and the CO_2 emission were calculated as complementary metrics. The optimal solution consists of a net profit of -$485 million USD/year, an Eco-Indicator 99 value of approximately 1.75 billion ecopoints/year, social welfare valued at 367.19, the creation of 15,488 jobs annually, and CO2 emissions of 2.2 kg CO2 per kg of products. This solution proposes replacing up to 6.43% of jet fuel with a hybrid system that includes four complete refineries and two pretreatment depots.

1. Introduction

Currently, the world is facing a series of problems derived from human activity and a linear economic model, such as climate change, deforestation, pollution, droughts, overpopulation, and a growing demand for energy. These issues have severe impacts on the environment, industrial development, as well as on society and the well-being of the population. For those reasons, it is not surprising that different governments, industries, and researchers are focusing on implementing sustainable practices to mitigate these effects. Such has been the interest of different countries and governments that in 2015, the United Nations General Assembly established the Sustainable Development Goals (SDGs), also known as UN 2030 agenda [1,2]. These consist of 17 points that address issues to be resolved in the short and medium term concerning social, economic, and environmental matters. These objectives are aimed at addressing various issues such as poverty, reducing inequalities, sustainable development of cities, action against climate change, among others [2].

On the other hand, the COVID-19 pandemic has shown that it is necessary to achieve these sustainable development goals as soon as possible, as it has severely impacted the fossil fuel industry, while renewable energy has become more cost-effective than ever before. Owing to the countries are focusing on economic recovery, they are prioritizing clean energy, viewing it as the "most cost-effective" investment [3,4]. Additionally, the use of renewable energy can drive sustainable economic growth and environmental improvements, boost a country's global image, and create opportunities for international trade with eco-friendly nations [3,4]. Thus, advocating for renewable energy usage can foster economic prosperity, improve environmental

* Corresponding author.
E-mail address: gcontreras@xanum.uam.mx (G. Contreras-Zarazúa).

https://doi.org/10.1016/j.cep.2024.110078
Received 15 December 2023; Received in revised form 23 September 2024; Accepted 19 November 2024
Available online 22 November 2024

Nomenclature

Sets

$i \in I$	Compounds
$j \in J$	Harvest Sites
$k \in K$	Pretreatment Depots
$l \in L$	Biorefineries
$m \in M$	Markets
$t \in T$	Time Periods

Subsets

I^{RM}	Raw Materials
I^{Int}	Intermediate Products (Ethanols, Ethylene)
I^{P}	Final Products (Gasolines, Biojet-fuel, Diesel)

Binary Variables

$y0^{RM}_{j,i}$	binary variable to enable the integration of biomass i from harvesting center j
$y1^{RM}_{j,i,l}$	Binary variable to control the shipment of biomass i from harvesting center j to the biorefinery l
$y3^{Int}_{i,k,l}$	binary variable to enable the shipment of fermentable sugars from pretreatment depot k to biorefinery l.
$y4^{Int}_{i,k,m}$	binary variable to enable the shipment of ethanol from pretreatment depot k to market m
$y5_{k}$	binary variable to enable the installation of the pretreatment depot
$y6^{Int}_{i,l,m}$	binary variable to enable the shipment of ethanol from biorefinery l to market m
$y7^{P}_{i,l,m}$	binary variable to enable the shipment of final product i from biorefinery l to market m
$y8_{l}$	binary variable to enable the installation of the biorefinery l
$y9^{Int}_{i,k,n=1}$	binary variable that controls y-intercept ($bCDP^{Int}_{i,n}$) when a pretreatment depot k is installed
$y10^{Int}_{i,l,n}$	binary variable that controls the value of the y-intercept ($bCRI^{Int}_{i,n}$) when biorefinery l is installed
$y11^{P}_{i,l,n}$	binary variable biorefinery l is installed

Parameters

$\gamma^{RM}_{i,t}$	Loss factor due to biomass degradation
$Disp^{RM}_{j,i,t}$	Biomass availability i in the harvest site j at time t (Ton)
$CHsDPU$	Maximum capacity for producing fermentable sugars in pretreatment depots (Ton/yr)
$EtOHDPU$	Maximum capacity for ethanol production in pretreatment depots (Ton/yr)
$EtOHRU$	Maximum capacity for ethanol production in biorefineries (Ton/yr)
$C2H4RU$	Maximum capacity for ethylene production in biorefineries (Ton/yr)
PRU	Maximum capacity for production of final products in biorefineries (Ton/yr)
$CapR^{L}$	Minimum ethanol processing capacity in biorefineries (Ton/yr)
$CapR^{U}$	Maximum processing capacity in biorefineries (Ton/yr)
$CapDP^{L}$	Minimum processing capacities of dry biomass in pretreatment depots (Ton/yr)
$CapDP^{U}$	Maximum processing capacities of dry biomass in pretreatment depots (Ton/yr)
$xCCDP^{Int}_{i,k,n}$	Annual production capacity of the pretreatment depot k for the intermediate product i, which falls within an interval n (Ton/yr)
$xCCRI^{Int}_{i,l,n}$	Annual production capacity of the intermediate product i of biorefinery l, (Ton/yr)
$xCCRP^{P}_{i,l,n}$	Annual production capacity of the final product i of biorefinery l that falls within an interval n (Ton/yr)
$RImin^{Int}_{i}$	Minimum production capacities of the intermediate product i in the biorefineries, among which $xCCRI^{Int}_{i,l,n}$ falls. (Ton/yr)
$RImed^{Int}_{i}$,	Medium production capacities of the intermediate product i in the biorefineries, among which $xCCRI^{Int}_{i,l,n}$ falls. (Ton/yr)
$RImax^{Int}_{i}$	Maximum production capacities of the intermediate product i in the biorefineries, among which $xCCRI^{Int}_{i,l,n}$ falls. (Ton/yr)
$RPmin^{P}_{i}$	Minimum production capacities of the final product i in the biorefineries, among which $xCCRP^{P}_{i,l,n}$is included. (Ton/yr)
$RPmed^{P}_{i}$	Medium production capacities of the final product i in the biorefineries, among which $xCCRP^{P}_{i,l,n}$is included. (Ton/yr)
$RPmax^{P}_{i}$	Maximum production capacities of the final product i in the biorefineries, among which $xCCRP^{P}_{i,l,n}$is included. (Ton/yr)
CB^{RM}_{i}	Cost per ton of biomass *I (USD/ton)*
$mCDP^{Int}_{i,n}$	Slope parameters for piecewise function to estimate capital costs of pretreatment depots.
$mCRI^{Int}_{i,n}$	Slope parameters for piecewise function to estimate capital costs of biorefineries for the stages of hydrolysis of biomass, the fermentation and separation of ethanol
$mCRP^{P}_{i,n}$	Slope parameters for piecewise function to estimate capital costs of biorefineries for the stages of ethylene and jet fuel production.
$mSDP^{Int}_{i}$	Slope parameters for piecewise function to estimate utilities costs of the pretreatment depot k
$mSRI^{Int}_{i}$	Slope parameters for piecewise function to estimate utilities costs of the biorefinery l for the production of intermediate products
$mSRP^{P}_{i}$	Slope parameters for piecewise function to estimate utilities costs of the biorefinery l to produce final products
$bCDP^{Int}_{i,n}$	y-intercept for piecewise function to estimate capital costs of pretreatment depots
$bCRI^{Int}_{i,n}$	y-intercept for piecewise function to estimate capital costs of biorefineries, for the stages of hydrolysis of biomass, the fermentation and separation of ethanol.
$bCRP^{P}_{i,n}$	y-intercept for piecewise function to estimate capital cost of biorefineries, for the stages of ethylene and jet fuel production.
$bSDP^{Int}_{i}$	y-intercept for piecewise function to estimate utilities costs of pretreatment depots k
$bSRI^{Int}_{i}$	y-intercept for piecewise function to estimate utilities costs of biorefinery l for the production of intermediate products
$bSRP^{P}_{i}$	y-intercept for piecewise function to estimate utilities costs of biorefinery l to produce final products
$D1^{RM}_{j,i,l}$	Distances from harvesting center j to biorefinery l and pretreatment depot k for biomass i, (Km)
$D2^{RM}_{j,i,k}$	Distances from harvesting center j to biorefinery l
$D3_{k,l}$	Distance from the pretreatment depot k to the biorefinery l (Km)
$D4_{k,m}$	Distances from the pretreatment depot k to the market m (Km)
$D5_{l,m}$	Distances from the the biorefinery l to the market m (Km)
$\eta^{RM,Int}_{i',i}$	Conversion factor from biomass i' to fermentable sugars
$\eta 1^{Int}_{i,i}$	Conversion factor from fermentable sugars to ethanol
$\eta 2^{Int}_{i,i}$	Conversion factor from ethanol to ethylene
$\eta^{Int,P}_{i',i}$	Conversion factor from ethylene to gasoline, biojet-fuel,

diesel, and heavy oils

$JGBU^{Direct}$ Multiplier for the generation of direct jobs at harvest sites by the use of biomass.

$JGBU^{Indirect}$, Multiplier for the generation of indirect jobs at harvest sites by the use of biomass.

$JGBU^{Induced}$ Multiplier for the generation of inducedirect jobs at harvest sites by the use of biomass.

JGT^{Direct} Direct jobs created during the transportation activities

$JGT^{Indirect}$, Direct jobs created during the transportation activities

$JGT^{Induced}$ Induced jobs created during the transportation activities

$JGOF^{Direct}$, Direct jobs created during the construction and operation of biorefineries

$JGOF^{Indirect}$ Indirect jobs created during the construction and operation of biorefineries

$JGOF^{Induced}$ Induced jobs created during the construction and operation of biorefineries

$C02factor$ emission factor for CO_2 by transportation

Variables

$ABCC^{RM}_{j,i,t}$ Storage of biomass i in the harvest center j at time t

$ABCC^{RM}_{j,i,t-1}$ Storage of biomass at the previous period of time t

$BER^{RM}_{j,i,l,t}$ Biomass sent to the biorefinery l from harvest site j (Ton)

$BEDP^{RM}_{j,i,k,t}$ Biomass sent to the pretreatment depot k from harvest site j (Ton)

$CBCC_{j,i,t}$ Consumption of biomass i in the harvest center j (Ton)

$CBDP^{RM}_{i,k,t}$ Biomass i processed at pretreatment depot k at time t

$CBDP^{RM}_{Sugar,k,t}$ Consumption of sugarcane bagasse at pretreatment depot k at time t

$CBDP^{RM}_{Corn,k,t}$ Consumption of corn at pretreatment depot k at time t

xS Percentage for the consumption of sugarcane bagasse

xC Percentage for the consumption of corn stover

$CHsDP^{Int}_{i,k,t}$ Fermentable sugars produced in pretreatment depot k at time t

$CHsOHDP^{Int}_{i,k,t}$ Fermentable sugars produced at time t that will continue their Processing at pretreatment depot k

$CHsER^{Int}_{i,k,l,t}$ Sugars sent to biorefinery l from pretreatment depot k

$EtOHDP^{Int}_{i,k,t}$ ethanol produced in pretreatment depot k at time t,

$EtOHER^{Int}_{i,k,l,t}$ ethanol produced at time t that is sent to biorefinery l

$EtOHEDPM^{Int}_{i,k,m,t}$ ethanol sent from pretreatment depot k to market m at time t

$CBR^{RM}_{i,l,t}$ Consumption of biomass i in biorefinery l at time t

$CBR^{RM}_{Sugar,l,t}$ consumption of sugarcane bagasse in biorefinery l at time t

$CBR^{RM}_{Corn,l,t}$ consumption of corn stover l at time t

$CHsPR^{Int}_{i,l,t}$ consumption of biomass i in biorefinery l at time t,

$CBR^{RM}_{Sugar,l,t}$ consumption of sugarcane bagasse

$CBR^{RM}_{Corn,l,t}$ consumption of corn stover

$CHsPR^{Int}_{i,l,t}$ fermentable sugars produced in biorefinery l at time t.

$CHsTR^{Int}_{i,l,t}$ total fermentable sugars present in biorefinery l at time t.

$EtOHR^{Int}_{i,l,t}$ ethanol produced in biorefinery l at time t.

$EtOHTR^{Int}_{i,l,t}$ total ethanol in biorefinery l at time

$OHC2H4^{Int}_{i,l,t}$ ethanol produced in biorefinery l at time t that continues its processing into ethylene

$EtOHERM^{Int}_{i,l,m,t}$ ethanol sent to market m

$C2H4R^{Int}_{i,l,t}$ ethylene produced in biorefinery l at time t,

$C2H4PF^{Int}_{i,l,t}$ ethylene produced in bio-refinery l at time t which undergoes further processing into jet-fuel

$C2H4ERM^{Int}_{i,l,m,t}$ ethylene sent to market m

$PPR^{P}_{i,l,t}$ final product i produced in biorefinery l at time t

$PERM^{P}_{i,l,m,t}$ final product i produced in biorefinery l that is sent to market m at time t

$h0^{RM}_{j,i,t}$ the bilinear product $DBCC^{RM}_{j,i,t} \cdot y0^{RM}_{j,i}$

$DPIM^{Int}_{i,m,t}$ demand for intermediate product i in market m at time t

$DPM^{P}_{i,m,t}$ demand for final product i in market m at time t

CMP Cost of the raw material used throughout the entire time horizon

$CTMP$ calculation of the transport cost for raw materials

$CTPI$ calculation of the transport cost for intermediate products

$CTPM$ calculation of the transport cost for products to market

$CF1$ fixed and for biomass transport

$CV1$ Carriable costs for biomass transport

$CF2$ fixed for fermentable sugars transport

$CV2$ variable costs for fermentable sugars transport

CUI the unit cost for the transport of flammable liquids

$CCDP_k$ capital cost of the pretreatment depot k, calculated from the linear equation of a specific interval n

$CCRI$ capital cost for the first three stages of the process in biorefinery l

$CCRP_l$ capital cost for the final stage of the process in biorefinery l.

$CSDP^{Int}_{i,k}$ Utility cost of the pretreatment depot k for the production of the intermediate product i,

$CSRI^{Int}_{i,l}$ utility costs of the biorefinery l for the production of intermediate products

$CSRP^{P}_{i,l}$ utility costs of the biorefinery l for the production of final products

VPI represents the revenue from the sale of intermediate products

VPF revenue from the sale of final products

PV_I selling price per ton of product i,

$EIDP^{Int}_{i,k}$ EI99 for the annual production of intermediate product i in pretreatment depot

$EIRI^{Int}_{i,l}$ EI99 for the annual production of intermediate product i in biorefinery l

$EIRP^{P}_{i,l}$ EI99 for the annual production of final product i

$iEIMP$ environmental impact of biomass use

$EITMP$ impact of raw material transportation

$EITPI$ intermediate product transportation environmental impact

$IBS^{P}_{i,m,t}$ social welfare index for each airport at time t which is a dimensionless number ranging from 0 to 1

conditions, and contribute to achieving the Sustainable Development Goals (SDGs).

It is important to highlight, that to achieve this energy transition requires changes in lifestyles, commodities production and consumption, as well as a considerable investment in the development of new innovative technologies, and infrastructure [5]. These changes and new technologies will allow to increase the efficiency of energy use, reduces waste generation, and decreases harmful emissions. In this sense, the process intensification can be a fundamental tool for achieving this transition to a more sustainable industry and society. Traditionally, Process Intensification (PI) has been defined as a concept that seeks safer processes, with very high equipment efficiencies, reducing the size and operating costs of equipment, as well as generating the least possible amount of waste and obtaining the greatest number of products with less consumption of raw materials, resulting in cheaper and more sustainable technologies [6,7]. While the traditional approach to process intensification can be useful for generating more efficient, cheaper, safer processes with lower environmental impacts compared to traditional

processes, this typical approach is still not enough to meet the objectives of sustainable development. The sustainability of a process is a multi-faceted issue. It does not solely rely on the efficiency of the processes themselves. Instead, sustainability is also influenced by other external factors. These factors, although not directly be part of the process, have a significant impact on its overall sustainability. Some of these factors include limitations in resources (availability, location, seasonality), regulatory barriers, financial and social constraints, among others [5]. Due to this, the concept and definition of process intensification have been evolving, not only to focus on the process itself but also to consider other factors such as scale, and artificial intelligence issues that play an important role in the development and sustainability of processes and products [8,9]. In order to effectively address these factors, the new research on process intensification has started to use new tools from Industry 4.0 such as Artificial Intelligence (AI), big data and analytics, supply chain simulation and modeling, smart manufacturing as well as new real-time optimization techniques and supply chain design [8,9]. The integration of these technologies, tools and approaches, coupled with process intensification, has been called as Process Intensification 4.0 (PI4.0) [8]. The objective of PI4.0 is to efficiently and intelligently coordinate networks of modules to meet the needs of end-users while adhering to various environmental constraints [8]. Therefore, PI can be viewed as a fundamental reevaluation of a process, aimed at significantly enhancing its overall efficiency and achieving a flexible, modular approach to distributed manufacturing [5,8,10]. Currently, there are few studies that have addressed the intensification of 4.0 processes to improve the efficiency and operations of a process. Villicaña-García et al., [9] proposed a mathematical model based on 4.0 intensification for the optimal utilization and reutilization of water during the shale gas production process. Their also model considers a modular and decentralized production and storage system, as well as the ability to consider the effect of different restrictions based on laws and regulations. Their results indicate that with a suitable decentralized schemes and economic incentive schemes the costs for water reutilization can be reduced up to 98.6%. Bhosekar and Ierapetritou [11] studied the modular design of different cases of study using a machine Learning-based flexibility analysis coupled with processes design modelling and optimization. The objective of their work was to demonstrate as modular based design has numerous benefits, including higher flexibility of decisions, lower investment costs, shorter time-to-market, and adaptability to market conditions. This modeling approach can be applied to both conventional and intensified processes such as reactive distillation, demonstrating that significant improvements in process sustainability can be achieved without complex mass and energy integrations (typical intensification), but simply by switching to a modular structure. López-Guajardo et al., [8] defined some approaches and tools that process intensification should use to achieve more sustainable industries and to transition more quickly towards a circular economy system. They concluded that the key focus of Process Intensification 4.0 should be on developing systems that are modular, interoperable, and decentralized. This approach is aimed at fostering an interconnected environment. Such a setup enhances understanding and facilitates the design or redesign of more efficient equipment, thereby driving a shift towards sustainable practices and a circular economy, especially in chemical processes. To successfully implement this, Artificial Intelligence, particularly Machine Learning, and mathematical modeling play a crucial role. They are essential for extracting information, recognizing patterns, and making predictions in this context.

As previously mentioned, studies in 4.0 process intensification are limited. Therefore, the options for applying this new approach are vast. In this regard, this approach can be especially attractive for biofuel production, specifically to produce renewable aviation fuel. The interest in this biofuel and its development is primarily due to the challenges associated with electrifying the aviation sector, which include issues such as battery efficiency and weight [12]. The International Air Transport Association (IATA) reported that in 2018, 4.4 billion passengers were transported by air, along with 63.7 million tons of cargo, equivalent to 35% of global trade by value [12]. As a consequence, the aviation industry is responsible for 2-3% of global carbon dioxide (CO_2) emissions by the year 2022 [13,14]. Additionally, it is expected to double its size and emissions by 2050, representing a 700% increase in CO_2 emissions since 2005. For these reasons, the aviation industry has explored different alternatives and technologies to reduce its pollutant emissions, with the most attractive option being the shift from conventional petroleum-derived jet fuel to sustainable aviation fuel (SAF), also called biojet fuel [12,13].

Nowadays, there are six recognized methods for producing biojet fuel for commercial flights: Fischer-Tropsch (FT), Hydroprocessed Esters and Fatty Acids (HEFA), Fischer-Tropsch with Aromatics (FT-SPK/A), Co-processing of renewable lipids, and Alcohol to Jet (ATJ) [14]. Among these technologies, the alcohol to Jet pathway is particularly notable due to its capability to utilize a broad spectrum of biomasses such as agricultural wastes and alcohols for jet fuel production. Additionally, alcohols are abundantly produced, providing logistical flexibility in the production process [15,16]. The Alcohol to Jet process (ATJ) involves six stages: biomass pretreatment, sugars hydrolysis and fermentation, alcohol dehydration, olefin oligomerization, hydrogenation, and hydrocarbon separation. Despite the advantages of the ATJ process, it has several challenges that need to be addressed to achieve its effective industrial implementation. Some of the challenges include low conversion yields from raw materials to alcohols, high energy consumption, and the availability and seasonality of biomass, which could limit its implementation. With this in mind, several research have been focused on improving the ATJ process. Romero-Izquierdo et al. [17] proposed using thermally coupled distillation configurations and heat integration to improve the energy efficiency of the ATJ. Their results show that these configurations, coupled with heat integration, can achieve energy savings of up to 34.75% in contrast to conventional process. Meanwhile, Contreras-Zarazua et al. [18] proposed a reactive distillation column for the oligomerization zone of the ATJ process, which drastically reduces the number of equipment required in the process. Their results indicate that the reactive distillation column offers cost savings of 20% while the reduction in environmental impact and safety is 50% and 22% respectively. Their results also indicate that the column can be operated using both feedback control systems and predictive optimal control. On the other hand, Huerta-Rosas et al. [19]proposed the intensification of different stages of the ATJ process. They used a simultaneous hydrolysis and fermentation reactor to intensify the alcohol production zone. At the same time, they considered the intensification of ethanol purification using a divided wall column and oligomerization and hydrogenation using a double reactive distillation column. Their results indicate that this fully intensified process has overall cost and environmental reductions of around 20% compared to the conventional process.

Rivas-Interian et al. [16] designed various intensified systems for ATJ production, including options such as vapor side stream distillation columns, dividing wall columns, as well as the use of different lignocellulosic residues to achieve a combination of raw materials and technologies that minimize the environmental impact of the process. The intensified alternatives were designed using the method of stochastic optimization known as differential evolution with a tabu list. The results show that savings of 5.56% and a reduction of 1.72% in Eco-indicator-99 were achieved with a vapor side stream column compared to conventional distillation. Meanwhile, with a dividing wall column, savings of 5.02% and reductions of 2.92% in Eco-indicator-99 were achieved. They concluded that this process is capable of meeting a demand required by Mexico exceeding 266 million liters of biojet fuel per year.

On the other hand, authors like Said et al. [20] proposed the use of alternative raw materials such as microalgal biomass to replace typical raw materials like lignocellulosic residues or oil crops. In their study, the production of biojet fuel using microalgae is evaluated. This production is assessed using two predictive models, the ANFIS-based model

(Adaptive Neuro-Fuzzy Inference System) and the RSM-based model (Response Surface Methodology). It was found that ANFIS outperformed RSM in terms of accuracy and predictive efficiency, achieving better correlation coefficients and lower uncertainty. Using the desirability technique, the ideal operational parameters were determined, resulting in a maximum yield of 91% in the production of microalgae oil methyl ester (AOME). Additionally, it was confirmed that the thermophysical properties of the produced fuel are comparable to those of standard Jet A-1 kerosene.

In the specific case of Mexico, the ATJ route is an interesting alternative to replace fossil jet fuel with SAF in its operations, due to the abundant resources, waste generation, and cultivable areas with high potential that Mexico possesses [16]. According to the Mexican Ministry of Agriculture (SAGARPA), the country produces an estimated 586 million tons of lignocellulosic residues from its 20 million hectares of agricultural land [21]. However, less than 5% of this biomass is currently used, mainly as cattle feed. The majority of the remaining residues are burned, which results in various environmental issues, including pollution, fires, and unregulated emissions [21]. Even though converting agricultural waste into SAF holds significant promise, there are notable challenges to be addressed for large-scale production. These challenges primarily revolve around the availability, accessibility, and geographical distribution of the biomass required for this process [16, 19,22]. The availability of biomass changes due to factors such as harvest location, season, soil nutrients, weather conditions, and farmers' planting decisions, among others. These drawbacks raise several queries about the sustainability of the process, as the costs and environmental impact of collecting and distributing biomass to refineries due to the biomass seasonality and variability could be greater than those of using fossil-based jet fuel. In addition, this variability can result in inconsistent fuel production, posing challenges in meeting the demand requirements [23].

Based on the aforementioned, this study explores the economic, environmental, and social feasibility of producing biojet fuel in Mexico using agricultural wastes and the Alcohol-to-Jet (ATJ) technology. The novel aspect of our research is the implementation of the "Process Intensification 4.0" approach. This innovative strategy evaluates the availability, seasonality, and geographical distribution of raw materials alongside the demand in various markets such as airports and stations. A distinctive feature of this research is the development of a sophisticated mathematical model that facilitates the decision-making process regarding the number and location of production plants, and the selection of appropriate raw materials. This model compares two systems: a centralized production system where the entire biojet fuel production is consolidated at a single site, and a decentralized, modular system that spreads production across multiple locations. The mathematical model was formulated as a multiperiod Mixed Integer Linear Programming (MILP). To determine the most sustainable option, the model employs an optimization technique that simultaneously considers net profit, environmental impact, and social impact as objective functions in order to address the three pillars of sustainability [24]. Economically, the goal is to maximize net profit; environmentally, impacts are quantified using the Eco-indicator 99; socially, impacts are measured using the Social Welfare Index to assess the equitable distribution of biojet fuel. Additionally, the model calculates CO_2 emissions and job creation in the biojet fuel supply chain and considers the commercial potential of intermediate products like ethanol and ethylene to enhance operational flexibility. This type of comprehensive analysis is essential for advancing towards the Sustainable Development Goals (SDGs) outlined in the 2030 Agenda, specifically Goals 7 (Affordable and Clean Energy), 9 (Industry, Innovation, and Infrastructure), 12 (Responsible Consumption and Production), and 13 (Climate Action). By addressing these goals, the study contributes significantly to sustainable development, promoting energy efficiency, innovation, environmental protection, and social equity through the development of sustainable biofuel production technologies.

2. Problem statement

Due to the large amount of agricultural waste produced in Mexico, this study has focused on the use and reuse of corn stover and sugarcane bagasse, owing to their high availability, as they are the most produced industrial agricultural residues in Mexico [23]. The yearly availability and costs of these agricultural residues are detailed in Table 1. Furthermore, Fig. 1 shows availability of corn stover and sugarcane bagasse in each Mexican state during different seasons.

As previously mentioned, this model considers the ATJ route as the technology for biojet- fuel production. It is important to highlight, that this route has the capability of using several types of alcohols for biojet-fuel production. However, in this case, ethanol is considered as the intermediary alcohol due to it is the most widely produced and available alcohol. Therefore, the ATJ process considered in this work consists of the following stages:

- Sugar fermentation: This stage comprises the pretreatment and fermentation of sugar to process produce ethanol.
- Ethanol dehydration: In this stage, ethanol is converted into ethylene through a catalytic step.
- Oligomerization, hydrogenation and separation: In this stage, ethylene is oligomerized to produce heavier molecular weight olefins (alkenes) within the bio jet-fuel range (C8 to C16). Subsequently, these olefins undergo a catalytic hydrogenation process to be converted into paraffins (alkanes), which are then separated into different fractions. The primary products obtained from these stages include gasoline, jet fuel, diesel, and heavy oils.

These three stages, which constitute the ATJ process, are considered the fundamental steps of the process and are the steps used for its modularization. In order to offer more flexibility a decentralized a modular structure was considered. This means that all products or conversions are not required to be shipment or produced at a single processing plant, or biorefinery. Instead, intermediate products can be produced at smaller facilities as well. Therefore, the mathematical model can consider performing these three stages in a single location or carrying them out in different locations, to improve the sustainability of the process (see Fig. 2a). Additionally, the model takes into account the production of valuable intermediate compounds like ethanol and ethylene, along with the creation of high-value co-products such as gasoline and diesel. The potential for commercializing these products is also considered. The supplementary material contains detailed data, including the geographical coordinates (latitude and longitude) of locations, as well as the demand levels of each market for these intermediate products. This information, due to its extensive nature, is presented in Tables S1 to S3 in the supplementary material. This model was developed with the objective of meeting Mexico's biojet-fuel requirements in the short to medium term. In this sense, according to data from the Secretary of Energy and the Secretary of Communications and Transportation of Mexico, Mexico should replace at least 5.5% of its demand with biojet-fuel by 2023, which is equivalent to 258 million liters of SAF [25,26]. On the other hand, as the maximum percentage to cover, a maximum of 50% of the national demand was established. This value was taken as an upper limit because, for safety reasons, biojet fuel must be mixed at a maximum of 50% with fossil jet fuel [27]. Fig. 2b shows all the locations of the most important airports in Mexico [25,26]. The demand of biojet-fuel for each airport is presented in the Table S4 of

Table 1
Availability and cost of corn stover and sugarcane bagasse. (Data from; SADER, [48] and SAGARPA, [21])

Lignocellulosic residue	Cost USD/Ton	Total Availability (Ton/year)
Corn stover	58.5	30,536,508
Sugarcane bagasse	25	19,224,167

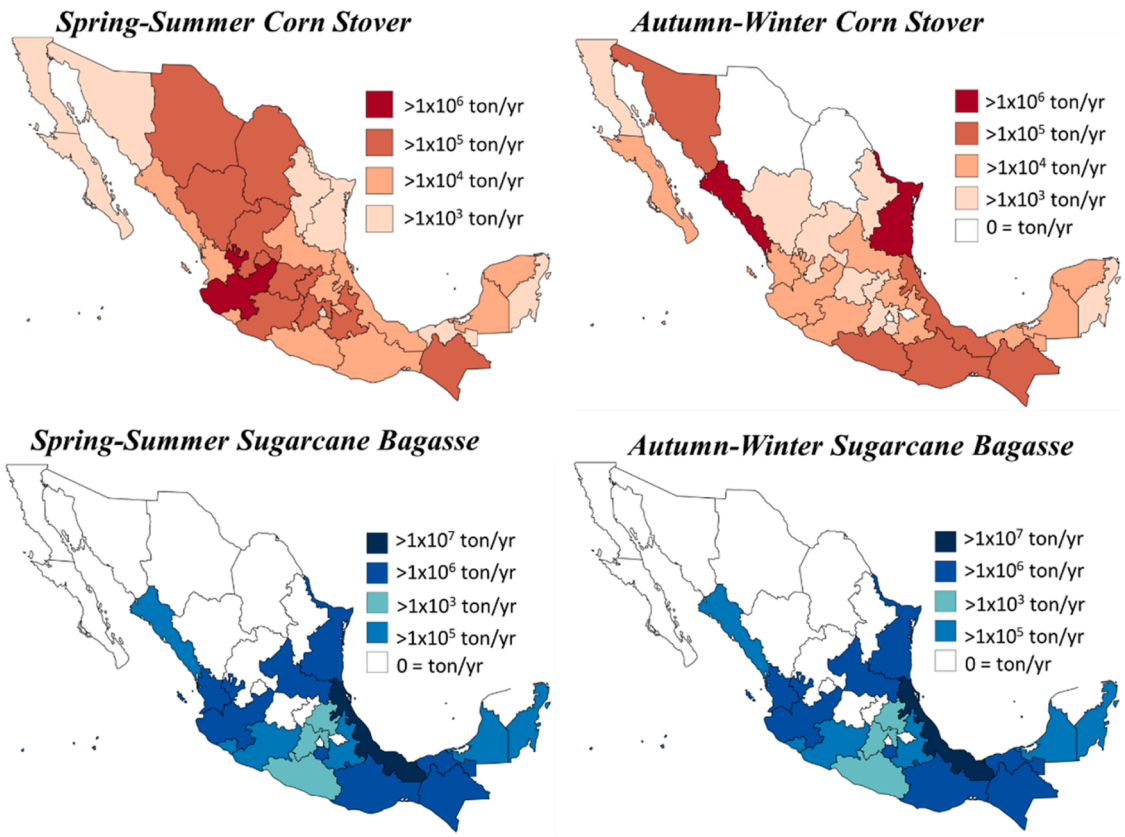

Fig. 1. Map for availability of corn stover and sugarcane bagasse in Mexico.

the supplementary material.

This model addresses the variability in biomass due to different harvest locations and seasonal changes through a multiperiod inventory planning approach within a one-year time horizon, divided into twelve different time periods (t∈T), each corresponding to a month of the year. This multiperiod planning is designed to effectively manage the storage and transportation of biomass and products, ensuring the continuous fulfillment of market demand [13,18]. The yields, energy requirements, costs, and environmental impacts per kilogram of biojet fuel produced in each step of the ATJ process were taken from the previous research conducted by Rivas-Interián [16]. These data are presented in the Table S5 of the supplementary material. Fig. 3 shows the superstructures considered for this model. where solid lines represent the centralized configuration, while dashed lines represent the decentralized configuration.

3. Model assumptions

This paper considers some assumptions in order to simplify the problem's modeling and solution. It is assumed that the centroid each state generated during the discretization of Mexico(see Fig. S1 of supplementary material).) is the place where all the lignocellulosic wastes of the state are located. Consequently, this point is considered as the harvest location. This assumption could be easily relaxed only dividing each discretization zone into smaller subsites [23]. The date of biomass availability in each centroid are showed in Tables S6 and S7 of supplementary material. Similarly, the potential locations for processing facilities were considered in these regions, with a distance of 10 km and 30 km from the centroid for pretreatment depots (k), dehydratation facilities and biorefineries (l), respectively. This assumption modelling is according to the reported by Contreras-Zarazúa et al. [23]. The coordinates for harvest sites and the different parts of the process are presented in the Table S8.

Additionally, it was assumed that biomass could only be stored at the harvest centers, considering a monthly degradation factor of 1.7% for sugarcane bagasse and 1.5% for corn stover [28,29]. Biomass degradation was presumed to occur only before transportation and was independent of its location, hence the same loss factors were applied to all harvest centers.

Lastly, to ensure supply certainty of SAF, considering that it is a product targeted at a highly specific market, the establishment of a cyclical inventory was proposed to mitigate seasonal availability and annual biomass variability. A cyclical inventory aims to maintain the same inventory level for the storage of raw materials and products at the beginning ($t = 0$) and end ($t = T$) of a time horizon, ensuring reproducibility of supply chain planning between different time horizons.

4. Model formulation

As aforementioned, the mathematical model was formulated as multiperiod Mixed Integer Lineal Programing (MILP) problem to consider the biomass seasonality. It is important to highlight, that the calculation of the transportation distances was carried out using the Rhum line method which is explained in the supplementary material. It is important to mention, that this model was developed for this case of study, it is based on material balance equations. Therefore, it can be extended to other types of biomasses or wastes, and it can be applicable to other countries by simply changing the capacity and transportation constraints as well as the locations. However, it is important to note that applying this model to other types of biomass requires specific data on production costs, yields, and conversions, as the composition and structure of each biomass affect these parameters. This means that, before conducting a similar study, a biorefinery design that considers the use of other biomasses must be available. Similar models can be found in the previous works reported by [28,29].

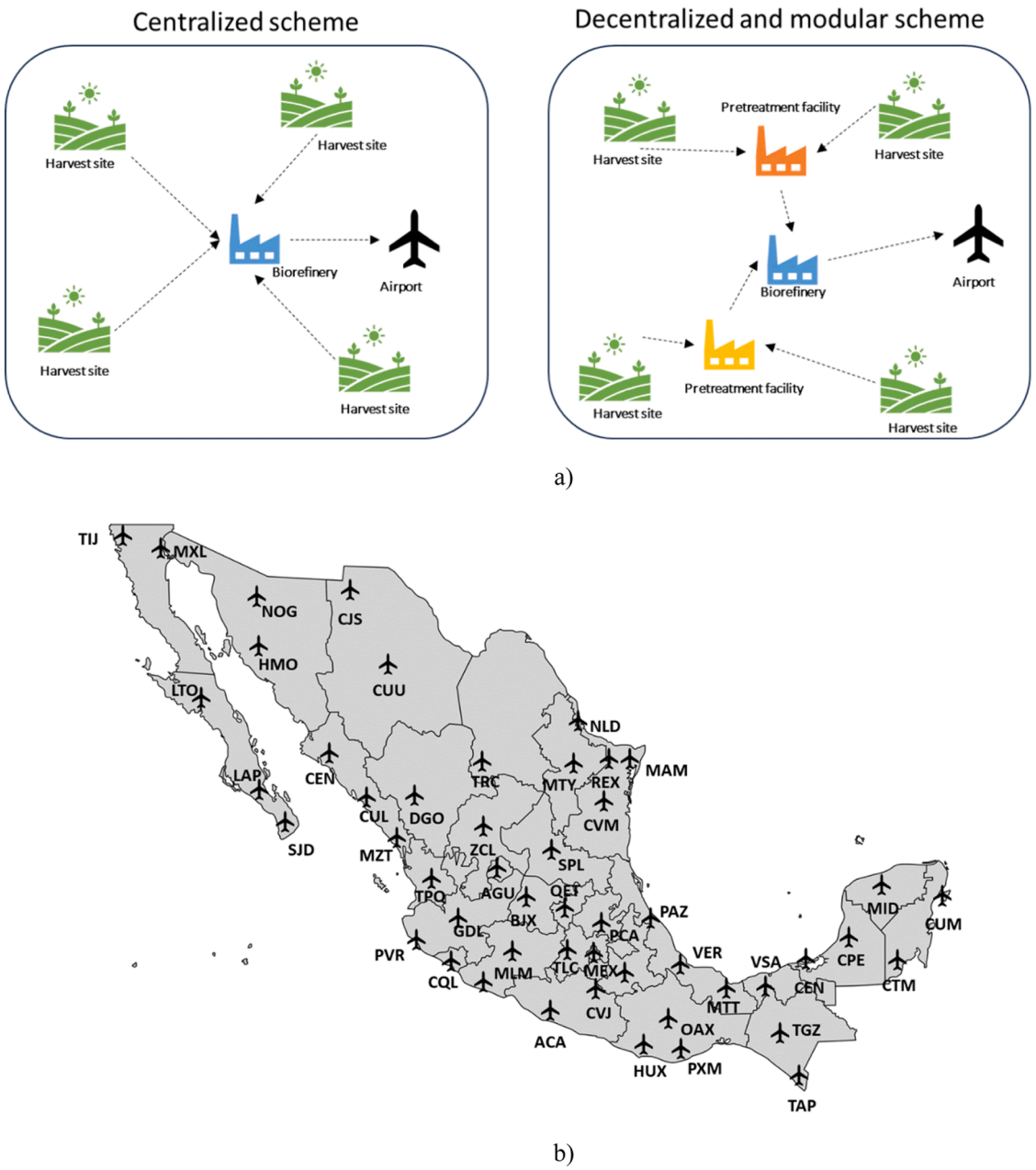

Fig. 2. a) Centralized and decentralized modular scheme b) Location of the main airports in Mexico

4.1. Harvest centers

Eq. 1 presents the material balance for calculating the storage of agricultural residue (*i*) in the harvest center (*j*) at time *t*.

$$ABCC_{j,i,t}^{RM} = ABCC_{j,i,t-1}^{RM}\left(1-\gamma_{i,t}^{RM}\right) + CBCC_{j,i,t}^{RM} - \sum_{l} BER_{j,i,l,t}^{RM} - \sum_{k} BEDP_{j,i,k,t}^{RM}\ i \in I^{RM}, j, t \quad (1)$$

$ABCC_{j,i,t}^{RM}$ is the storage of biomass *i* in the harvest center *j* at time *t*, while $ABCC_{j,i,t-1}^{RM}$ is the storage at the previous time. $\gamma_{i,t}^{RM}$ is the biomass loss factor due to degradation, $BER_{j,i,l,t}^{RM}$ is the biomass sent to the biorefinery *l* from harvest site *j*, and $BEDP_{j,i,k,t}^{RM}$ is the biomass sent to the pretreatment depot *k*. Lastly, $CBCC_{j,i,t}$ is the consumption of biomass *i* in the harvest center *j*, which is constrained by the biomass availability ($Disp_{j,i,t}^{RM}$) as shown in Eq. 2.

$$CBCC_{j,i,t}^{RM} \leq Disp_{j,i,t}^{RM}\ i \in I^{RM}, j, t \quad (2)$$

On the other hand, biomass shipments to processing facilities are restricted in accordance with the following Eq. 3:

$$\sum_{t} BER_{j,i,l,t}^{RM} \leq \sum_{t} Disp_{j,i,t}^{RM} \cdot y1_{j,i,l}^{RM}\ i \in I^{RM}, j, l \quad (3)$$

Where $y1_{j,i,l}^{RM}$ is the binary variable for the selection of biomass *i* from harvesting center *j* to the biorefinery *l*. If $y1_{j,i,l}^{RM}$=1 the shipment of biomass from from harvesting center *j* to the biorefinery *l* is selected, otherwise it is not chosen.

The cyclic inventory considers that the biomass stored at the end of the final period (t=T) matches the amount stored at the start of the initial period (t=0), which ensures a constant supply of biomass to the processing facilities. The cyclic inventory can be mathematically represented as follows:

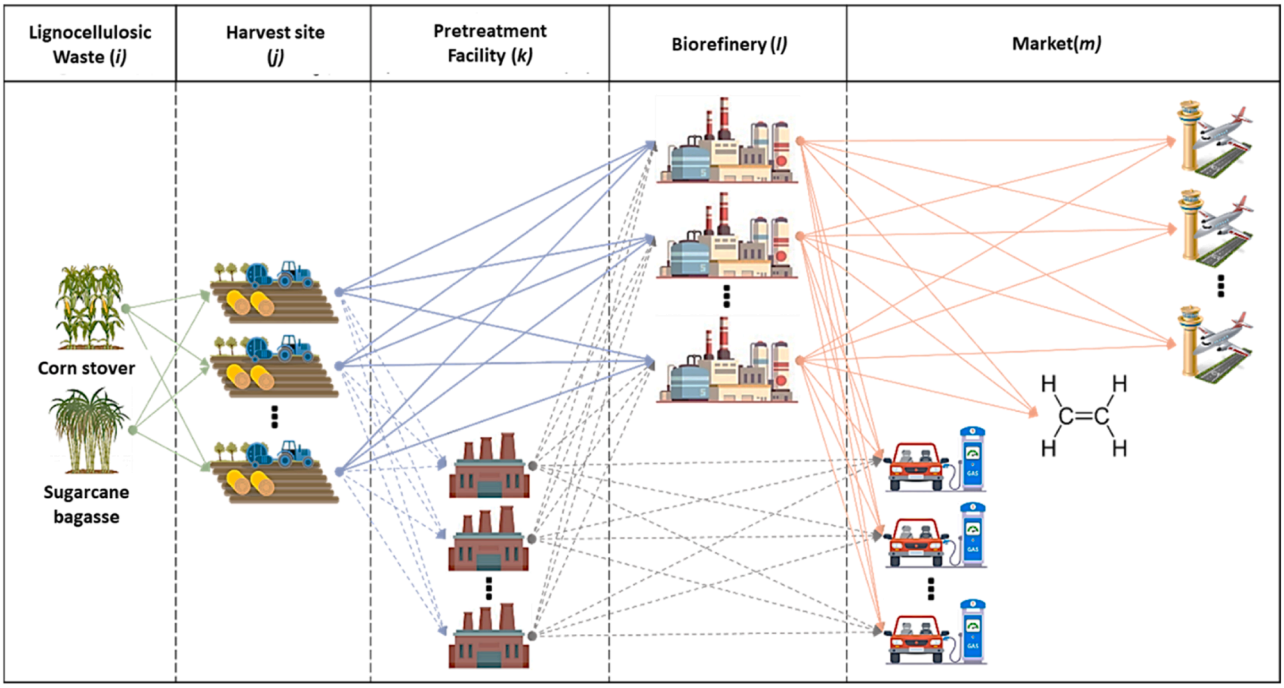

Fig. 3. Superstructure for producing biojet-fuel suing ATJ route.

$$ABCC^{RM}_{j,i,t=0} = ABCC^{RM}_{j,i,t=T}\ i \in I^{RM}, j, t \tag{4}$$

4.2. Pretreatment depots

The objective of the pretreatment centers is to convert biomass into more energy-dense products (ethanol and fermentable sugars) to reduce transportation costs. In this regard, Eq. 5 represents the biomass arriving from the harvest centers to the pretreatment depots.

$$CBDP^{RM}_{i,k,t} = \sum_{j} BEDP^{RM}_{j,i,k,t}\ i \in I^{RM}, k, t \tag{5}$$

Where $CBDP^{RM}_{i,k,t}$ is the biomass i processed at pretreatment depot k at time t. The conversion data from different raw materials to more dense products are expressed in Equations 6 and Eq. 6.

$$CBDP^{RM}_{Sugar,k,t} = xS \sum_{i} CBDP^{RM}_{i,k,t}\ Sugar \in I^{RM}, k, t \tag{6}$$

$$CBDP^{RM}_{Corn,k,t} = xC \sum_{i} CBDP^{RM}_{i,k,t}\ Corn \in I^{RM}, k, t \tag{7}$$

Where, $CBDP^{RM}_{Sugar,k,t}$and $CBDP^{RM}_{Corn,k,t}$ represent the consumption of sugarcane bagasse and corn stover, respectively. On the other hand, xS and xC represent the percentage for the consumption of sugarcane bagasse and corn stover in processing facilities. These equations represent the constrains required to ensure the parallel processing of sugarcane bagasse and corn stover.

Eq. 8 presents the production of fermentable sugars from sugarcane bagasse and corn stover in the pretreatment depot.

$$CHsDP^{Int}_{i,k,t} = \sum_{i' \in RM} \eta^{RM,Int}_{i',i} \cdot CBDP^{RM}_{i',k,t}\ i \in I^{Int}, k, t \tag{8}$$

$CHsDP^{Int}_{i,k,t}$ represents the fermentable sugars produced in pretreatment depot k at time t, while $\eta^{RM,Int}_{i',i}$ is the conversion factor from biomass i' to fermentable sugars as presented in Table S5 of the supplementary material. Although fermentable sugars have a higher energy density than biomass, their storage was not considered as they are still susceptible to degradation. It is important to mention that these sugars can continue their processing in the same pretreatment facility or be sent to refineries for further processing. Eq. 9 presents the mass balance for fermentable sugars in the pretreatment depot.

$$CHsDP^{Int}_{i,k,t} = CHsOHDP^{Int}_{i,k,t} + \sum_{l} CHsER^{Int}_{i,k,l,t}\ i \in I^{Int}, k, t \tag{9}$$

Where $CHsOHDP^{Int}_{i,k,t}$ represents the fermentable sugars produced at time t that will continue their processing on-site, while $CHsER^{Int}_{i,k,l,t}$ represents the sugars sent to biorefinery l to continue the processing. The following equation represent the constrain for the shipment of fermentable sugars from pretreatment depot k to biorefinery l:

$$CHsER^{Int}_{i,k,l,t} \leq CHsDPU \cdot y3^{Int}_{i,k,l}\ i \in I^{Int}, k, l, t \tag{10}$$

Where $y3^{Int}_{i,k,l}$ is the binary variable to enable the shipment of fermentable sugars from pretreatment depot k to biorefinery l. $CHsDPU$ is the maximum capacity for producing fermentable sugars in pretreatment depots.

The conversion of fermentable sugars that continue their processing (conversion to ethanol) in the pretreatment depot can be expressed as follows:

$$EtOHDP^{Int}_{i,k,t} = \eta 1^{Int}_{i,i} \cdot CHsOHDP^{Int}_{i,k,t}\ i \in I^{Int}, k, t \tag{11}$$

Where $EtOHDP^{Int}_{i,k,t}$ is the ethanol produced in pretreatment depot k at time t, while $\eta 1^{Int}_{i,i}$ is the conversion factor from fermentable sugars to ethanol as presented in Table S5 of the supplementary material. As aforementioned, this ethanol can be sent to the biorefinery to continue its processing or directly marketed from the pretreatment depot as an oxygenate for gasoline. Eq. 12 presents the mass balance for ethanol in the pretreatment depot.

$$EtOHDP^{Int}_{i,k,t} = \sum_{l} EtOHER^{Int}_{i,k,l,t} - \sum_{m} EtOHEDPM^{Int}_{i,k,m,t}\ i \in I^{Int}, k, t \tag{12}$$

Where $EtOHER^{Int}_{i,k,l,t}$ is the ethanol produced at time t that is sent to biorefinery l to continue its processing, while $EtOHEDPM^{Int}_{i,k,m,t}$ is the ethanol sent from pretreatment depot k to market m at time t. The following equation is the constrain for the shipment of ethanol from pretreatment depot k to biorefinery l:

$$\sum_t EtOHER^{Int}_{i,k,l,t} \le EtOHDPU \cdot y3^{Int}_{i,k,l}\ i \in I^{Int}, k, l \tag{13}$$

where now $y3^{Int}_{i,k,l}$ is the binary variable to enable the shipment of ethanol from pretreatment depot k to biorefinery l and $EtOHDPU$ is the maximum capacity for ethanol production in pretreatment depots.

The shipment of ethanol from pretreatment depot k to market m was restricted as shown below:

$$\sum_t EtOHEDPM^{Int}_{i,k,m,t} \le EtOHDPU \cdot y4^{Int}_{i,k,m}\ i \in I^{Int}, k, m \tag{14}$$

Where $y4^{Int}_{i,k,m}$ is the binary variable to enable the shipment of ethanol from pretreatment depot k to market m.

4.3. Biorefineries

As part of the operation of biorefineries, it was considered that they could start their operation from the processing of biomass as well as from the processing of fermentable sugars or ethanol sent from the pretreatment depots. The following equations present the biomass storage in the biorefineries:

$$CBR^{RM}_{i,l,t} = \sum_j BER^{RM}_{j,i,l,t}\ i \in I^{RM}, l, t \tag{15}$$

$$CBR^{RM}_{Sugar,l,t} = xS \sum_i CBR^{RM}_{i,l,t}\ Sugar \in I^{RM}, l, t \tag{16}$$

$$CBR^{RM}_{Corn,l,t} = xC \sum_i CBR^{RM}_{i,l,t}\ Corn \in I^{RM}, l, t \tag{17}$$

$CBR^{RM}_{i,l,t}$ represents the consumption of biomass i in biorefinery l at time t, while $CBR^{RM}_{Sugar,l,t}$ and $CBR^{RM}_{Corn,l,t}$ represent the consumption of sugarcane bagasse and corn stover, respectively. It is important to highlight that this work is based on a previous study reported by Rivas-Interián et al., [16] in which a multi-objective optimization was performed to determine the conditions of the ATJ process that minimize both the environmental impact and the costs of the process. In that sense, the optimal ratio of sugarcane bagasse and corn stover to be fed into the process was determined. Eqs. 16 and 17 ensure that this ratio is maintained.

In the case where the biorefinery operates with biomass, the transformation of this into fermentable sugars is given by Eq. 18

$$CHsPR^{Int}_{i,l,t} = \sum_{i' \in RM} \eta^{RM,Int}_{i',i} \cdot CBR^{RM}_{i',l,t}\ i \in I^{Int}, l, t \tag{18}$$

Where $CHsPR^{Int}_{i,l,t}$ represents the fermentable sugars produced in biorefinery l at time t. On the other hand, considering that the biorefinery can receive sugars from pretreatment depots as well as work with sugars produced in the same refineries. Eq. 19 represents the mass balance for fermentable sugars in the biorefinery.

$$CHsTR^{Int}_{i,l,t} = CHsPR^{Int}_{i,l,t} + \sum_k CHsER^{Int}_{i,k,l,t}\ i \in I^{Int}, l, t \tag{19}$$

Where $CHsTR^{Int}_{i,l,t}$ represents the total fermentable sugars present in biorefinery l at time t. This equation considers the sum of fermentable sugars that may come from pretreatment depots and those produced in the biorefinery. These sugars can be converted into ethanol. Eq. 20 represents this conversion from fermentable sugar to ethanol:

$$EtOHR^{Int}_{i,l,t} = \eta 1^{Int}_{i,i} \cdot CHsTR^{Int}_{i,l,t}\ i \in I^{Int}, l, t \tag{20}$$

Where $EtOHR^{Int}_{i,l,t}$ is the ethanol produced in biorefinery l at time t. However, similar to fermentable sugars, the operation of the biorefinery can also start from the processing of ethanol sent by the pretreatment depots. Therefore, Eq. 21 presents the mass balance for ethanol in the biorefinery.

$$EtOHTR^{Int}_{i,l,t} = EtOHR^{Int}_{i,l,t} + \sum_k EtOHER^{Int}_{i,k,l,t}\ i \in I^{Int}, l, t \tag{21}$$

$EtOHTR^{Int}_{i,l,t}$ represents the total ethanol in biorefinery l at time t. This ethanol produced in refineries has two possible destinations: being sold to an end market or being sent for transformation into ethylene. This can be expressed mathematically according to Eq. 22

$$EtOHTR^{Int}_{i,l,t} = OHC2H4^{Int}_{i,l,t} + \sum_m EtOHERM^{Int}_{i,l,m,t}\ i \in I^{Int}, l, t \tag{22}$$

Where $OHC2H4^{Int}_{i,l,t}$ is the ethanol produced in biorefinery l at time t that continues its processing into ethylene, while $EtOHERM^{Int}_{i,l,m,t}$ is the ethanol sent to market m, which was restricted as shown in the following equations:

$$\sum_t EtOHERM^{Int}_{i,l,m,t} \le EtOHRU \cdot y6^{Int}_{i,l,m}\ i \in I^{Int}, l, m, t \tag{23}$$

Where $EtOHRU$ is the maximum capacity for ethanol production in biorefineries and $y6^{Int}_{i,l,m}$ is the binary variable to enable the shipment of ethanol from biorefinery l to market m.

Once the ethanol market output is considered, the remaining ethanol is processed into ethylene as shown in Eq. 24.

$$C2H4R^{Int}_{i,l,t} = \eta 2^{Int}_{i,i} \cdot OHC2H4^{Int}_{i,l,t}\ i \in I^{Int}, l, t \tag{24}$$

$C2H4R^{Int}_{i,l,t}$ represents the ethylene produced in biorefinery l at time t, while $\eta 2^{Int}_{i,i}$ is the conversion factor from ethanol to ethylene as presented in Table S5 of the supplementary material. As mentioned, the market output of ethylene as a chemical block was also considered. Therefore, Eq. 309 presents the mass balance for ethylene in the biorefinery.

$$C2H4R^{Int}_{i,l,t} = C2H4PF^{Int}_{i,l,t} + \sum_m C2H4ERM^{Int}_{i,l,m,t}\ i \in I^{Int}, l, t \tag{25}$$

$C2H4PF^{Int}_{i,l,t}$ is the ethylene produced in bio-refinery l at time t, which undergoes further processing into jet-fuel, while $C2H4ERM^{Int}_{i,l,m,t}$ is the ethylene sent to market m, with restricted output as shown below:

$$\sum_t C2H4ERM^{Int}_{i,l,m,t} \le C2H4RU \cdot y6^{Int}_{i,l,m}\ i \in I^{Int}, l, m, t \tag{26}$$

Where $C2H4RU$ is the maximum capacity for ethylene production in biorefineries, and now $y6^{Int}_{i,l,m}$ is the binary variable to enable the shipment of ethylene from biorefinery l to market m.

Eq. 27 presents the production of biojet-fuel and by-products from the processing of ethylene in the biorefinery.

$$PPR^{P}_{i,l,t} = \eta^{Int,P}_{i',i} \cdot C2H4PF^{Int}_{i',l,t}\ i \in I^{P}, i' \in I^{Int}, l, t \tag{27}$$

Where $PPR^{P}_{i,l,t}$ represents the final products i produced in biorefinery l at time t, while $\eta^{Int,P}_{i',i}$ is the conversion factor from ethylene to gasoline, biojet-fuel, diesel, and heavy oils as presented in Table S5 of the supplementary material. However, only the market output of gasoline, bioturbosine, and diesel was considered, and its mass balance is presented in Eq. 28.

$$PPR^{P}_{i,l,t} = \sum_m PERM^{P}_{i,l,m,t}\ i \in I^{P}, l, t \tag{28}$$

$PERM^{P}_{i,l,m,t}$ represents the final product i produced in biorefinery l that is sent to market m at time t, and its market output was restricted as shown below:

$$\sum_t PERM^{P}_{i,l,m,t} \le PRU \cdot y7^{P}_{i,l,m}\ i \in I^{P}, l, m \tag{29}$$

Here, represents PRU is the maximum capacity for production of final products in biorefineries whereas $y7^{P}_{i,l,m}$is the binary variable to enable the shipment of final product i from biorefinery l to market m.

5. Model constraints

5.1. Capacity constrains for pretreatment depots

Given that the primary function of the pretreatment depots is the densification of biomass, the operation of these facilities was restricted by their biomass processing capacity, as shown below in Eq. 30:

$$\boldsymbol{CapDP^{L}}\cdot \boldsymbol{y5_{k}} \leq \sum_{i\in RM}\sum_{t} \boldsymbol{CBDP^{RM}_{i,k,t}} \leq \boldsymbol{CapDP^{U}}\cdot \boldsymbol{y5_{k}}\ \boldsymbol{k} \tag{30}$$

Where $y5_k$ is the binary variable to enable the installation of the pretreatment depot, while $CapDP^L$ and $CapDP^U$ are respectively the minimum and maximum processing capacities of dry biomass in pretreatment depots.

Considering that the maximum aspiration of these facilities is the commercialization of the produced ethanol. $CapDP^U$ was taken as 165,000 tons/year in accordance with the minimum biomass processing reported by Hernández et al., [30] to ensure economically competitive ethanol production, while $CapDP^L$ was arbitrarily taken as 10% of $CapDP^U$, that is, 16,500 tons/year.

5.2. Capacity constrains for biorefineries

Since the operation of the biorefineries is related to the reception of biomass, fermentable sugars, and/or ethanol, their operation was restricted by the ethanol processing capacity as shown below in Eq. 51:

$$\boldsymbol{CapR^{L}}\cdot \boldsymbol{y8_{l}} \leq \sum_{i\in Int}\sum_{t} \boldsymbol{EtOHTR^{Int}_{i,l,t}} \leq \boldsymbol{CapR^{U}}\cdot \boldsymbol{y8_{l}}\ \boldsymbol{l} \tag{31}$$

Where $y8_l$ is the binary variable to enable the installation of the biorefinery l where the ethanol produced on-site or received from the pretreatment depots will be processed. $CapR^L$ is the minimum ethanol processing capacity in biorefineries, taken as 25,628 tons/year, the ethanol equivalent of the minimum processing reported by Hernández et al., (2019), while $CapR^U$ is the maximum processing capacity taken as 1,591,109 tons/year, the ethanol resulting from processing all the available sugarcane bagasse in Mexico and the respective amount of corn stover

5.3. Connectivity constrains

Considering that the interaction between nodes occurs through the flow of biomass, intermediate products, and final products, these flows were restricted to provide connectivity only to the network of harvesting centers, pretreatment depots, biorefineries, and markets that made up the supply chain design.

The following equations present the restrictions used to ensure that the harvesting centers included in the supply chain design provided biomass to the processing facilities, as well as to ensure that the biomass was consumed and not stored unjustifiably.

$$\boldsymbol{DBCC^{RM}_{j,i,t}} - \sum_{t} \boldsymbol{Disp^{RM}_{j,i,t}}\left(1-\boldsymbol{y0^{RM}_{j,i}}\right) \leq \boldsymbol{h0^{RM}_{j,i,t}}\ \boldsymbol{i}\in \boldsymbol{I^{RM}}, \boldsymbol{j}, \boldsymbol{t} \tag{32}$$

$$\boldsymbol{h0^{RM}_{j,i,t}} \leq \boldsymbol{DBCC^{RM}_{j,i,t}}\ \boldsymbol{i}\in \boldsymbol{I^{RM}}, \boldsymbol{j}, \boldsymbol{t} \tag{33}$$

$$\boldsymbol{h0^{RM}_{j,i,t}} \leq \sum_{t} \boldsymbol{Disp^{RM}_{j,i,t}}\cdot \boldsymbol{y0^{RM}_{j,i}}\ \boldsymbol{i}\in \boldsymbol{I^{RM}}, \boldsymbol{j}, \boldsymbol{t} \tag{34}$$

$$\sum_{k} \boldsymbol{BEDP^{RM}_{j,i,k,t}} + \sum_{l} \boldsymbol{BER^{RM}_{j,i,l,t}} \leq \boldsymbol{h0_{j,i,t}}\ \boldsymbol{i}\in \boldsymbol{I^{RM}}, \boldsymbol{j}, \boldsymbol{t} \tag{35}$$

Here, $h0^{RM}_{j,i,t}$ represents the bilinear product $DBCC^{RM}_{j,i,t}\cdot y0^{RM}_{j,i}$, with $y0^{RM}_{j,i}$ being the binary variable to enable the integration of biomass i from harvesting center j into the supply chain. Meanwhile, Eq. 35, while considering the degradation of biomass due to storage, aims to ensure that the biomass integrated into the supply chain is processed in pretreatment depots and/or biorefineries.

The following equations show how the shipment of intermediate products from the pretreatment depot k, as well as the shipment of both intermediate and final products from the biorefinery l, was controlled:

$$\boldsymbol{y3^{Int}_{i,k,l}} \leq \boldsymbol{y5_{k}} \tag{36}$$

$$\boldsymbol{y4^{Int}_{i,k,m}} \leq \boldsymbol{y5_{k}} \tag{37}$$

$$\boldsymbol{y6^{Int}_{i,l,m}} \leq \boldsymbol{y8_{l}} \tag{38}$$

$$\boldsymbol{y7^{P}_{i,l,m}} \leq \boldsymbol{y8_{l}} \tag{39}$$

In this case, the shipment arcs $k\rightarrow l$, $k\rightarrow m$, and $l\rightarrow m$ were restricted to ensure that there is a flow of material through them, provided that the pretreatment depot k and/or the biorefinery l are considered within the supply chain design.

Similarly, the integration of the supply chain with the existing infrastructure for the storage, distribution, and production of both intermediate and final products occurred through the window defined by the demand for each of these products, these data are showed in the Tables is presented in Table S8 of supplementary material. In the case of the following equations present the restrictions used to prevent the shipment of products to the market from exceeding its demand.

$$\sum_{k} \boldsymbol{EtOHEDPM^{Int}_{i,k,m,t}} + \sum_{l} \boldsymbol{EtOHERM^{Int}_{i,l,m,t}} \leq \boldsymbol{DPIM^{Int}_{i,m,t}}\ \boldsymbol{i}\in \boldsymbol{I^{Int}}, \boldsymbol{m}, \boldsymbol{t} \tag{40}$$

$$\sum_{l} \boldsymbol{C2H4ERM^{Int}_{i,l,m,t}} \leq \boldsymbol{DPIM^{Int}_{i,m,t}}\ \boldsymbol{i}\in \boldsymbol{I^{Int}}, \boldsymbol{m}, \boldsymbol{t} \tag{41}$$

$$\sum_{l} \boldsymbol{PERM^{P}_{i,l,m,t}} \leq \boldsymbol{DPM^{P}_{i,m,t}}\ \boldsymbol{i}\in \boldsymbol{I^{P}}, \boldsymbol{m}, \boldsymbol{t} \tag{42}$$

Here, $DPIM^{Int}_{i,m,t}$ is the demand for intermediate product i in market m at time t, while $DPM^{P}_{i,m,t}$ is the demand for final product i in market m at time t.

Lastly, Eq. 43 presents the way in which the coverage of the lower limit for the demand for jet fuel in Mexico was controlled, which considered covering 5.5% of the jet fuel consumption at each storage station.

$$\sum_{l} \boldsymbol{PERM^{P}_{i,l,m,t}} \geq 0.055\cdot \boldsymbol{DPM^{P}_{i,m,t}}\ \boldsymbol{i}\in \boldsymbol{I^{P}}, \boldsymbol{m}, \boldsymbol{t} \tag{43}$$

6. Transportation and raw material costs

The price of agricultural waste is primarily associated with its collection, with the volume of biomass being the only variable that significantly affects its cost. This was considered in the calculation of the total cost for biomass consumption as shown below in Eq. 44:

$$\boldsymbol{CMP} = \sum_{j}\sum_{i\in RM}\sum_{t} \boldsymbol{CB^{RM}_{i}}\cdot \boldsymbol{CBCC^{RM}_{j,i,t}} \tag{44}$$

Where CMP represents the cost of the raw material used throughout the entire time horizon of the supply chain, while CB^{RM}_i is the cost per ton of biomass i, which was presented in Table 1.

In the case of transportation costs, it was considered that transportation between harvesting centers, processing facilities, and markets would be by road, using cargo trucks and tankers for the transport of raw materials, intermediate products, and final products. This cost was calculated from the fixed and variable cost for transport by tractor-trailer, parameters reported in the literature that are a function of the load carried and the distance traveled. However, these are also often condensed into a parameter known as the unit cost of transport.

Next, Eq. 45 presents the calculation of the transport cost for raw materials ($CTMP$), Eq. 46 presents the calculation of the transport cost for intermediate products ($CTPI$), while Eq. 47 presents the calculation

of the transport cost for products to market *CTPM*).

$$CTMP = \sum_{j}\sum_{i\in RM}\sum_{l}\sum_{t} BER^{RM}_{j,i,l,t}\left(CF1 + CV1\cdot D1^{RM}_{j,i,l}\right) + \sum_{j}\sum_{i\in RM}\sum_{k}\sum_{t} BEDP^{RM}_{j,i,k,t}\left(CF1 + CV1\cdot D2^{RM}_{j,i,k}\right) \quad (45)$$

$$CTPI = \sum_{k}\sum_{l}\sum_{t} CHsER^{Int}_{i,k,l,t}\left(CF2 + CV2\cdot D3_{k,l}\right) + \sum_{k}\sum_{l}\sum_{t} EtOHER^{Int}_{i,k,l,t}\left(CUI\cdot D3_{k,l}\right) \quad (46)$$

$$CTPM = \sum_{i\in Int}\sum_{k}\sum_{m}\sum_{t} EtOHEDPM^{Int}_{i,k,m,t}\left(CUI\cdot D4_{k,m}\right) + \sum_{l}\sum_{m}\sum_{t}\left[\sum_{i\in Int}\left(EtOHERM^{Int}_{i,l,m,t} + C2H4ERM^{Int}_{i,l,m,t}\right) + \sum_{i'\in P} PERM^{P}_{i',l,m,t}\right]\left(CUI\cdot D5_{l,m}\right) \quad (47)$$

Where $D1^{RM}_{j,i,l}$ and $D2^{RM}_{j,i,k}$ are the distances from harvesting center j to biorefinery l and pretreatment depot k for biomass i, $D3_{k,l}$ is the distance from the pretreatment depot k to the biorefinery l, while $D4_{k,m}$ and $D5_{l,m}$ are the distances from the pretreatment depot k and the biorefinery l to the market m. *CF1* and *CV1* are the fixed and variable costs for biomass transport, *CF2* and *CV2* are the fixed and variable costs for fermentable sugars transport, while CUI is the unit cost for the transport of flammable liquids, which are presented in Table S.10 of supplementary material.

7. Calculation of capital and utilities costs

As part of the model, the process proposed by Rivas-Interián et al., [16] was divided into four stages: the first covered the pretreatment and hydrolysis of the biomass (E1), the second the fermentation and separation of ethanol (E2), the third the dehydration of ethanol into ethylene (E3), and the fourth both the oligomerization of ethylene, and the hydrogenation and separation of the resulting paraffinic mixture (E4).

Using the process of Rivas-Interián et al., [16] as a basis, each of these stages was scaled to three different plant sizes, calculating the cost of each through the Guthrie method, considering 8,500 operational hours per year and a return on investment period of 10 years. The purpose of this scaling was to obtain a continuous function to estimate the process cost of each stage under different operational capacities.

However, the capital cost function exhibits a nonlinear behavior, preventing its integration into the proposed MILP model in this work. Therefore, the capital cost function was simplified into a piecewise linear approximation approach according to the reported by Contreras-Zarazua et al., [23]. As aforementioned, the equations were obtained from simulating the process proposed by Rivas-Interián et al., [16] and estimating the costs of different sections of the process for different capacities. The equations obtained are showed below:

$$\sum_{n} xCCDP^{Int}_{i,k,n} = \sum_{t} CHsDP^{Int}_{i,k,t} \quad i\in I^{Int}, k \quad (48)$$

$$\sum_{n} xCCDP^{Int}_{i,k,n} = \sum_{t} EtOHPDP^{Int}_{i,k,t} \quad i\in I^{Int}, k \quad (49)$$

$$CCDP_k = \sum_{i\in Int}\sum_{n}\left(mCDP^{Int}_{i,n}\cdot xCCDP^{Int}_{i,k,n} + bCDP^{Int}_{i,n}\cdot y9^{Int}_{i,k,n}\right) \quad k \quad (50)$$

$$\sum_{i}\sum_{n} y9^{Int}_{i,k,n} = y5_k \quad k \quad (51)$$

$xCCDP^{Int}_{i,k,n}$ is the annual production capacity of the pretreatment depot k for the intermediate product i, which falls within an interval n. Meanwhile, $CCDP_k$ is the capital cost of the pretreatment depot k, calculated from the linear equation of a specific interval n, where $mCDP^{Int}_{i,n}$ is the slope and $bCDP^{Int}_{i,n}$ the y-intercept of the linear equation in that interval.

Note that the value of the slope is controlled by the variable $xCCDP^{Int}_{i,k,n}$, which can take a value of 0 in the case that the intermediate product i is not produced in the pretreatment depot k, while the value of the y-intercept ($bCDP^{Int}_{i,n}$) is controlled by the binary variable $y9^{Int}_{i,k,n}$, which can be activated as long as the pretreatment depot k is installed.

In Eqs. 52 and 53, the restrictions used both to place the value of the variable $xCCDP^{Int}_{i,k,n}$ within one of the intervals of the piecewise linear approximation and to ensure that this corresponds to the actual value of the variable are presented.

$$DPmin^{Int}_{i}\cdot y9^{Int}_{i,k,n=1} \le xCCDP^{Int}_{i,k,n=1} \le DPmed^{Int}_{i}\cdot y9^{Int}_{i,k,n=1} \quad i\in I^{Int}, k, n=1 \quad (52)$$

$$DPmed^{Int}_{i}\cdot y9^{Int}_{i,k,n=2} \le xCCDP^{Int}_{i,k,n=2} \le DPmax^{Int}_{i}\cdot y9^{Int}_{i,k,n=2} \quad i\in I^{Int}, k, n=2 \quad (53)$$

Where $DPmin^{min}_{i}$, $DPmed^{med}_{i}$, and $DPmax^{max}_{i}$ respectively represent the minimum, medium, and maximum production capacities of intermediate product i in the pretreatment depots, among which the value of $xCCDP^{Int}_{i,k,n}$ must be found.

Considering that the first three stages of the process cover the production of fermentable sugars, as well as ethanol and ethylene production, the following equations present the calculation of the capital cost for refineries for the pretreatment and hydrolysis of biomass, the fermentation and separation of ethanol, as well as the dehydration of ethanol into ethylene:

$$\sum_{n} xCCRI^{Int}_{i,l,n} = \sum_{t} CHsPR^{Int}_{i,l,t} \quad i\in I^{Int}, l \quad (54)$$

$$\sum_{n} xCCRI^{Int}_{i,l,n} = \sum_{t} EtOHPR^{Int}_{i,l,t} \quad i\in I^{Int}, l \quad (55)$$

$$\sum_{n} xCCRI^{Int}_{i,l,n} = \sum_{t} C2H4PR^{Int}_{i,k,t} \quad i\in I^{Int}, l \quad (56)$$

$$CCRI_l = \sum_{i\in Int}\sum_{n}\left(mCRI^{Int}_{i,n}\cdot xCCRI^{Int}_{i,l,n} + bCRI^{Int}_{i,n}\cdot y10^{Int}_{i,l,n}\right) \quad l \quad (57)$$

$$\sum_{n} y10^{Int}_{i,l,n} \le y8_l \quad l \quad (58)$$

Here, $xCCRI^{Int}_{i,l,n}$ is the annual production capacity of the intermediate product i of biorefinery l, which controls the value of the slope ($mCRI^{Int}_{i,n}$) of the linear equation in interval n, while $y10^{Int}_{i,l,n}$ is the binary variable that controls the value of the y-intercept ($bCRI^{Int}_{i,n}$) in case the biorefinery l is installed, with $CCRI_l$ being the capital cost for the first three stages of the process in biorefinery l.

In the following equations, the calculation of the capital cost for biorefineries for the oligomerization of ethylene, as well as the production of biojet-fuel, is presented:

$$\sum_{n} xCCRP^{P}_{i,l,n} = \sum_{t} PPR^{P}_{i,l,t} \quad i\in I^{P}, l \quad (59)$$

$$CCRP_l = \sum_{i\in P}\sum_{n}\left(mCRP^{P}_{i,n}\cdot xCCRP^{P}_{i,l,n} + bCRP^{P}_{i,n}\cdot y11^{P}_{i,l,n}\right) \quad l \quad (60)$$

$$\sum_{n} y11^{P}_{i,l,n} \le y8_l \quad i\in I^{P}, l \quad (61)$$

$xCCRP^{P}_{i,l,n}$ is the annual production capacity of the final product i of biorefinery l that falls within an interval n, while $mCRP^{P}_{i,n}$ and $bCRP^{P}_{i,n}$ are the slope and y-intercept of the linear equation in that interval, controlled by $xCCRP^{P}_{i,l,n}$ and the binary variable $y11^{P}_{i,l,n}$ in the event that

biorefinery l is installed. $CCRP_l$ is the capital cost for the final stage of the process in biorefinery l.

In Eqs. 62 and 63, the restrictions used to assign the value of the variable $xCCRI^{Int}_{i,l,n}$ to the corresponding interval n are presented

$$\boldsymbol{RImin}^{Int}_{i}\cdot \boldsymbol{y}10^{Int}_{i,l,n=1} \leq \boldsymbol{xCCRI}^{Int}_{i,l,n=1} \leq \boldsymbol{RImed}^{Int}_{i}\cdot \boldsymbol{y}10^{Int}_{i,l,n=1}\ \boldsymbol{i} \in \boldsymbol{I}^{Int}, \boldsymbol{l}, \boldsymbol{n}=1 \tag{62}$$

$$\boldsymbol{RImed}^{Int}_{i}\cdot \boldsymbol{y}10^{Int}_{i,l,n=2} \leq \boldsymbol{xCCRI}^{Int}_{i,l,n=2} \leq \boldsymbol{RImax}^{Int}_{i}\cdot \boldsymbol{y}10^{Int}_{i,l,n=2}\ \boldsymbol{i} \in \boldsymbol{I}^{Int}, \boldsymbol{l}, \boldsymbol{n}=2 \tag{63}$$

Where $RImin^{Int}_{i}$, $RImed^{Int}_{i}$, and $RImax^{Int}_{i}$ represent the minimum, medium, and maximum production capacities of the intermediate product i in the biorefineries, among which $xCCRI^{Int}_{i,l,n}$ falls.

Eqs. 64 and 65 present the way in which the value of the variable $xCCRP^{P}_{i,l,n}$ was bounded to be assigned to the correct interval of the piecewise linear approximation.

$$\boldsymbol{RPmin}^{P}_{i}\cdot \boldsymbol{y}11^{P}_{i,l,n=1} \leq \boldsymbol{xCCRP}^{P}_{i,l,n=1} \leq \boldsymbol{RPmed}^{P}_{i}\cdot \boldsymbol{y}11^{P}_{i,l,n=1}\ \boldsymbol{i} \in \boldsymbol{I}^{P}, \boldsymbol{l}, \boldsymbol{n}=1 \tag{64}$$

$$\boldsymbol{RPmed}^{P}_{i}\cdot \boldsymbol{y}11^{P}_{i,l,n=2} \leq \boldsymbol{xCCRP}^{P}_{i,l,n=2} \leq \boldsymbol{RPmax}^{P}_{i}\cdot \boldsymbol{y}11^{P}_{i,l,n=2}\ \boldsymbol{i} \in \boldsymbol{I}^{P}, \boldsymbol{l}, \boldsymbol{n}=2 \tag{65}$$

With $RPmin^{P}_{i}$, $RPmed^{P}_{i}$, and $RPmax^{P}_{i}$ being the minimum, medium, and maximum production capacities of the final product i in the biorefineries, among which $xCCRP^{P}_{i,l,n}$ is included.

Unlike the capital cost, the function obtained by scaling the process for the cost of utilities exhibited a linear behavior across the entire domain of the function, using the parameters of the linear equation in the calculation of the utility costs for processing facilities as shown below:

$$\boldsymbol{CSDP}^{Int}_{i,k} = \boldsymbol{mSDP}^{Int}_{i}\cdot\sum_{n}\boldsymbol{xCCDP}^{Int}_{i,k,n} + \boldsymbol{bSDP}^{Int}_{i}\cdot\sum_{n}\boldsymbol{y}9_{CHs,k,n}\ \boldsymbol{i} \in \boldsymbol{I}^{Int}, \boldsymbol{k} \tag{66}$$

$$\boldsymbol{CSRI}^{Int}_{i,l} = \boldsymbol{mSRI}^{Int}_{i}\cdot\sum_{n}\boldsymbol{xCCRI}^{Int}_{i,l,n} + \boldsymbol{bSRI}^{Int}_{i}\cdot\sum_{n}\boldsymbol{y}10^{Int}_{i,l,n}\ \boldsymbol{i} \in \boldsymbol{I}^{Int}, \boldsymbol{l} \tag{67}$$

$$\boldsymbol{CSRP}^{P}_{i,l} = \boldsymbol{mSRP}^{P}_{i}\cdot\sum_{n}\boldsymbol{xCCRP}^{P}_{i,l,n} + \boldsymbol{bSRP}^{P}_{i}\cdot\sum_{n}\boldsymbol{y}11^{P}_{i,l,n}\ \boldsymbol{i} \in \boldsymbol{I}^{Int}, \boldsymbol{l} \tag{68}$$

$CSDP^{Int}_{i,k}$ is the utility cost of the pretreatment depot k for the production of the intermediate product i, while $CSRI^{Int}_{i,l}$ and $CSRP^{P}_{i,l}$ are the utility costs of the biorefinery l for the production of intermediate and final products, respectively.

Eq. 69 presents the calculation of the process cost for processing facilities ($CPIP$), which represents the investment required for the operation of the pretreatment depots and biorefineries that formed the design of the supply chain.

$$\boldsymbol{CPIP} = \sum_{\boldsymbol{k}}\left(\boldsymbol{CCDP}_{\boldsymbol{k}} + \sum_{\boldsymbol{i}\in\boldsymbol{Int}}\boldsymbol{CSDP}^{Int}_{i,k}\right) + \sum_{\boldsymbol{l}}\left(\boldsymbol{CCRI}_{\boldsymbol{l}} + \boldsymbol{CCRP}_{\boldsymbol{l}} + \sum_{\boldsymbol{i}\in\boldsymbol{Int}}\boldsymbol{CSRI}^{Int}_{i,l} + \sum_{\boldsymbol{i'}\in\boldsymbol{P}}\boldsymbol{CSRP}^{P}_{i',l}\right) \tag{69}$$

The data used to estimate the capital and utilities costs are present in the Tables S.11-S.14 of supplementary material.

8. Objective functions

This section provides an explanation of the metrics used as objectives functions to measure the performance of the solution. The metrics chosen as objective functions werethe maximization of net profit, the Eco-indicator 99 and the Social Welfare. These metrics evaluate economic, environmental and social aspects of the scheme production. These criteria were chosen according to the three pillars of sustainability which are economic, environmental and social [31]. These metrics collectively ensure a thorough and balanced evaluation of the jet-fuel production economic viability, environmental sustainability, and social equity.

The metric of net profit allows to quantify the profitability of selling SAF at prices comparable to conventional jet fuel derived from petroleum, thereby revealing the economic efficiency of the production process and production scheme [32]. This metric not only aligns with the United Nations Sustainable Development Goal 7 [5]: Affordable and Clean Energy by highlighting the potential reductions in production costs, but it also enables the identification of process bottlenecks and areas needing improvement and more intensification to ensure economic viability. Additionally, this metric is useful to determine if the degree of intensification of a given process is adequate to achieve economic viability.

Concerning environmental impact, the Eco-Indicator 99 is a composite metric that evaluates a range of environmental effects across 11 categories [23,33], including climate change, resource depletion, and energy use. This indicator is particularly advantageous for integrating into multi-objective optimization frameworks due to its ability to summarize complex environmental data into a singular 'eco-point', facilitating a holistic assessment of both process-specific and broader macro-environmental impacts. Such comprehensive evaluation is essential to determine the operational models, from centralized to modular-distributed systems that minimize the environmental impact. Additionally, the integration of the Eco-indicator 99 is useful to address Goals 7, 9, 12 and 13, as it provides a comprehensive assessment of environmental impacts, which is crucial for promoting sustainable consumption and production patterns and for combating climate change.

In the case of social welfare, it serves as a crucial metric for assessing the equitable distribution of resources among stakeholders, crucial for ensuring that all parties, including smaller airports, benefit equitably from the production scheme. This metric is vital for assessing social equity and complements the economic and environmental evaluations by ensuring that the biofuel production is distributed equitably, reinforcing Goal 9 by promoting innovative and resilient infrastructure.

In addition to these three objective functions, two complementary metrics were evaluated: CO_2 emissions per ton of product and job creation resulting from the economic activities generated by the Alcohol-to-Jet (ATJ) production scheme. Job creation is calculated using the Jobs and Economic Development Impact (JEDI) methodology. These additional metrics provide further insights and contribute to a more comprehensive evaluation of each potential solution. It is important to note that while these indices are not treated as primary objective functions, they are assessed together with each solution to ensure a holistic decision-making process.

8.1. Economic metric: profit

As previously mentioned, the economic aspect considered for the model optimization was the maximization of net profit, which is the difference between the revenue from the sale of products in the market and the total cost of the supply chain of raw materials, products and as well as the operative and installation costs of the facilities. As the sale of products drives the economic objective function, Eqs. 89 and 90 present the calculation of revenue from the sale of intermediate and final products, respectively.

$$\boldsymbol{VPI} = \sum_{\boldsymbol{i}\in\boldsymbol{Int}}\sum_{\boldsymbol{m}}\sum_{\boldsymbol{t}}\boldsymbol{PV}^{Int}_{i}\left[\sum_{\boldsymbol{k}}\boldsymbol{EtOHEDPM}^{Int}_{i,k,mt} + \sum_{\boldsymbol{l}}\left(\boldsymbol{EtOHERM}^{Int}_{i,l,m,t} + \boldsymbol{C2H4ERM}^{Int}_{i,l,m,t}\right)\right] \tag{70}$$

$$\boldsymbol{VPF} = \boldsymbol{PV}_i^P \sum_{i\in P}\sum_{l}\sum_{m}\sum_{t}\boldsymbol{PERM}_{i,l,m,t}^P \tag{71}$$

Here, *VPI* represents the revenue from the sale of intermediate products, while *VPF* indicates the revenue from the sale of final products. PV_I is the selling price per ton of product *i*, with prices set at 518.08 USD for ethanol [34], 344.22 USD for ethylene [35], 1,314.76 USD for gasoline [36], 896.47 USD for biojet-fuel [36], and 1,148.61 USD for diesel [36].

The design of the supply chain does not account for product storage within the processing facilities. Instead, it relies on the existing storage and distribution infrastructure in the country. Thus, the prices listed earlier correspond to the first-hand selling price, which is the price at which petroleum products enter the storage stations of the Mexican government

Mathematically the profit can be expressed according with the next Eq.:

$$\max \boldsymbol{Profit} = \boldsymbol{VPF} + \boldsymbol{VPI} - \boldsymbol{CPIP} - \boldsymbol{CMP} - \boldsymbol{CTMP} - \boldsymbol{CTPI} - \boldsymbol{CTPM} \tag{72}$$

8.2. Environmental metric: eco-indicator 99 (EI99)

The environmental objective function is quantified using the Eco-Indicator-99 (EI99), a methodology based on a life cycle assessment proposed by Goedkoop and Spriensma [33]. The EI99 has proven to be a powerful tool for assessing the environmental impact of supply chains, having been successfully applied in several previous works [37–39]. This method quantifies the environmental impact of a specific process or activity by evaluating three main damage categories: damage to human health, damage to ecosystems, and resource depletion. In addition. In this work, a Hierarchist perspective is chosen to estimate the eco-indicator 99, as this perspective considers a balance between short- and long-term effects in the evaluation of environmental impact. From a Hierarchist perspective, the contribution to the total EI99 is distributed as follows: damage to human health and damage to ecosystem quality contribute 40% each, while resource depletion contributes 20% [33]. Given this, the damage factors of these three categories in the supply chain are known and are directly associated with the amount of substances, transportation distance, and the technology involved process involved. The parameters used to calculate the EI99 are reported by Contreras-Zarazua et al [23], Goedkoop and Spriensma [33], Russo et al., [40], and Santibañez-Aguilar et al., [41]. Finally, the objective function for EI99 can be expressed as follows:

$$\min \boldsymbol{EI}99 = \sum_{i\in Int}\sum_{k}\boldsymbol{EIDP}_{i,k}^{Int} + \sum_{l}\left(\sum_{i\in Int}\boldsymbol{EIRI}_{i,l}^{Int} + \sum_{i'\in P}\boldsymbol{EIRP}_{i',l}^{P}\right) + \boldsymbol{EIMP} + \boldsymbol{EITMP} + \boldsymbol{EITPI} + \boldsymbol{EITPM} \tag{73}$$

$EIDP_{i,k}^{Int}$ is the EI99 for the annual production of intermediate product *i* in pretreatment depot *k*. $EIRI_{i,l}^{Int}$ is the EI99 for the annual production of intermediate product *i* in biorefinery *l*, while $EIRP_{i,l}^{P}$ is the EI99 for the annual production of final product *i*. *iEIMP* is the environmental impact of biomass use, and finally, the impact of raw material transportation *EITMP*, intermediate product transportation *EITPI*, and market output transportation on the environment. The parameters used to calculate the EI99 are showed in Table S15

8.3. Social metric: social welfare

The social aspect considered in the optimization of the supply chain was addressed through the equitable distribution of biojet-fuel throughout the national territory. Therefore, considering that the allocation of finite resources is not a trivial task and is a fundamental problem in social planning, this work employed a social welfare scheme to address the distribution of biojet-fuel in Mexico.

The social welfare scheme has been employed in markets such as electricity, where supply and generation are allocated based on social welfare, as well as in the allocation of bandwidth in telecommunications networks or flow control in air traffic. It is the most used scheme in the field of engineering for resource allocation among multiple stakeholders [42].

In this work, the social dimension was integrated into the optimization of the supply chain to consider the effect of government initiatives that aim to transition to biofuels on the design of the supply chain. To prevent markets with higher demand from being favored over those with lower demand, social welfare considered a dimensionless demand for jet-fuel in each market, which is shown below in Eq. 74.

$$\boldsymbol{IBS}_{i,m,t}^{P} = \frac{\boldsymbol{DPM}_{i,m,t}^{P} - \sum_i \boldsymbol{PERM}_{i,l,m,t}^{P}}{\boldsymbol{DPM}_{i,m,t}^{P}} \quad \boldsymbol{i} \in \boldsymbol{I}^{P}, \boldsymbol{m}, \boldsymbol{t} \tag{74}$$

Here, $IBS_{i,m,t}^{P}$ is the social welfare index for each airport at time *t*, which is a dimensionless number ranging from 0 to 1. When the demand for jet-fuel in market *m* at time t is met, $IBS_{i,m,t}^{P} = 0$; otherwise, $IBS_{i,m,t}^{P} = 1$. In this way, the objective function presented in Eq. 75 considers the same demand for all markets, resulting in a more homogeneous coverage in terms of the distribution of available resources.

$$\min \boldsymbol{BS} = \sum_{i\in P}\sum_{m}\sum_{t}\boldsymbol{IBS}_{i,m,t}^{P} \tag{75}$$

To solve the multi-objective supply chain problem, the ε-constrained method was employed. This approach involves initially solving the Mixed Integer Linear Programming (MILP) for each objective separately, without considering the others, to establish their respective limits. Then, using these established limits, the multi-objective problem is addressed for each objective by treating the other objectives as constraints. Mavrotas [43] provides more detailed information about this technique

8.3.1. Complementary index: CO_2 emissions

For CO_2 emissions, the total CO_2 emitted is considered the sum of emissions from the different stages of biofuel production. This includes CO_2 emissions from transporting raw materials from the field to the biorefinery and pretreatment depots, CO_2 emissions from the various production facilities (pretreatment depots and biorefineries), and CO_2 emissions from transporting biofuels and products from the biorefineries and pretreatment depots to the markets [44]. These emissions ($C02emiss$) at each of the different stages can be mathematically expressed with the following set of equations:

$$\boldsymbol{C02emiss} = \sum_{k=1}\boldsymbol{CO_2PD}_k + \sum_{l=1}\boldsymbol{CO_2R}_{i,l} + \sum_{i=1}\boldsymbol{CO2TMP}_i^{RM} + \sum_{i=1}\boldsymbol{CO2TPI}_i^{Int} + \sum_{i=1}\boldsymbol{CO2TPM}_i^{P} \tag{76}$$

$$\boldsymbol{CO2TMP}_i^{RM} = (\boldsymbol{C02factor})\sum_{j=1}\sum_{k=1}\sum_{t=1}\left(\boldsymbol{D2}_{j,i,k}^{RM}\right)\boldsymbol{BEDP}_{j,i,k,t}^{RM} + (\boldsymbol{C02factor})\sum_{j=1}\sum_{l=1}\sum_{t=1}\left(\boldsymbol{D1}_{j,i,l}^{RM}\right)\boldsymbol{BER}_{j,i,l,t}^{RM} \tag{77}$$

$$\boldsymbol{CO2TPI}_i^{Int} = (\boldsymbol{C02factor})\sum_{k=1}\sum_{l=1}\sum_{t=1}\left(\boldsymbol{D3}_{k,l}\right)\boldsymbol{CHsER}_{i,k,l,t}^{Int} + \sum_{k=1}\sum_{l=1}\sum_{t=1}\left(\boldsymbol{D3}_{k,l}\right)\boldsymbol{EtOHER}_{i,k,l,t}^{Int} + +(\boldsymbol{C02factor})\sum_{k=1}\sum_{m=1}\sum_{t=1}\left(\boldsymbol{D4}_{k,m}\right)\boldsymbol{EtOHEDPM}_{i,k,m,t}^{Int} \tag{78}$$

$$\boldsymbol{CO2TPM_i^P} = (\boldsymbol{C02factor})\sum_{k=1}\sum_{l=1}\sum_{t=1}(\boldsymbol{D5_{l,m}})\boldsymbol{EtOHERM_{i,l,m,t}^{Int}} + \sum_{k=1}\sum_{l=1}\sum_{t=1}(\boldsymbol{D5_{l,m}})\boldsymbol{C2H4ERM_{i,l,m,t}^{Int}} + +(\boldsymbol{C02factor})\sum_{k=1}\sum_{m=1}\sum_{t=1}(\boldsymbol{D5_{l,m}})\boldsymbol{PERM_{i,l,m,t}^{P}}$$

Where, CO_2PD_k represents the CO_2 emissions from the operation of pretreatment depot k, CO_2R_l are the CO_2 emissions from the operation of biorefinery l. The CO_2 emissions for the pretreatment centers and biorefineries were obtained from the work of Rivas-Interian et al. [16], and the CO_2 emissions were calculated using the Net Heating Value (NHV) method, considering natural gas as the main energy source for the pretreatment and biorefinery facilities [45]. The CO_2 emissions were associated with the size of the plants using the Piecewise Linear Approximation technique, analogous to the costs. The equations for CO_2 emissions are found in Table S17 of the supplementary material.

$CO2TMP_i^{RM}$ represents the emissions from the transportation of raw materials, $CO2TPI_i^{Int}$ is the emissions from the transportation of intermediate products, $CO2TPM_i^P$ correspond to CO_2 emissions from the transportation of products to market. The *C02factor*, which is the emission factor for CO_2, is equivalent to 4.65×10^{-5} CO_2 Ton/tkm for 72-ton trucks [46].

8.3.2. Complementary index: Jobs Generated

The Jobs and Economic Development Impact (JEDI) index was included as complementary index to evaluate the social impact. This index was developed by the National Renewable Energy Laboratory (NREL). The JEDI index is an input-output model that uses multipliers to calculate how the influence of new economic activities, such as the installation of a plant, impacts the economy of a region. Particularly, this metric quantifies these economic impacts through job creation. This methodology estimates the total employment impact (number of jobs) generated by a project, based on an initial economic output. The jobs identified by this method are categorized into three types:

- Direct Jobs: These are jobs created directly on the project site, including all employment during the construction and operational phases of the project.
- Indirect Jobs: Jobs created outside the project site, involving roles in transportation, manufacturing, supply, and other supporting industries.
- Induced Jobs: These are jobs are created due to the economic activities generated by the project, typically through increased spending by employees from direct and indirect jobs.

In this study, the required multipliers were derived from the models provided by National Renewable Energy Laboratory. Mathematically, the JEDI model can be expressed as follows:

$$\begin{aligned} Jobs = {} & \left(JGBU^{Direct} + JGBU^{Indirect} + JGBU^{Induced}\right) * CPM \\ & + \left(JGT^{Direct} + JGT^{Indirect} + JGT^{Induced}\right) * CTMP \\ & + \left(JGP^{Direct} + JGT^{Indirect} + JGT^{Induced}\right) * CTPI \\ & + \left(JGOF^{Direct} + JGT^{Indirect} + JGT^{Induced}\right) * CPIP \end{aligned} \quad (79)$$

where $JGBU^{Direct}$, $JGBU^{Indirect}$, $JGBU^{Induced}$ are the multipliers for the generation of direct, indirect, and induced jobs at harvest sites by the use of biomass. JGT^{Direct}, $JGT^{Indirect}$, $JGT^{Induced}$ are the jobs created during the transportation activities (Jobs/million USD dollar). $JGOF^{Direct}$, $JGOF^{Indirect}$, $JGOF^{Induced}$, represents the multiplier of jobs created during the construction and operation of biorefineries, pretreatment depots. It is important to mention that all multipliers have units of jobs/USD because the JEDI methodology associates the level of investment or expenditure with job generation. Therefore, to use this methodology, it is necessary to calculate the costs associated with each and every single stage of the supply chain, which are calculated in the net profit objective function.

9. Results

In this section, the results obtained from the optimization of the supply chain model are presented. The model was formulated as a MILP model consisting of 15,056 binary variables, 512,266 continuous variables, and 836,227 equations. This model was solved using a computer system with a CPU Ryzen™ 5500 @4.2 GHz processor and 32GB of RAM @3200MHz, with computation times ranging from 3,000 to 29,000 seconds. The CPLEX solver was used with a relative gap of less 1% for all solutions presented in this section.

Fig. 4 shows the Pareto fronts for different combinations of objective functions. These Pareto fronts were generated from random sampling points using the Latin Hypercube Sampling (LHS) method [47]. The red point in the various Pareto front graphs represents the solution considered to have the best trade-off between the environmental and social metrics by the authors. It is important to note that these red points are the same solution expressed in different graphs. The values of net profit, environmental impact, social welfare, CO_2 emissions, and jobs created for this solution are shown in Table 2. On the other hand, the comparison between the different objective functions and the complementary indices is shown in Fig. 5.

To explain the results more clearly, we will begin by discussing the objective function of net profit in relation to other objective functions and complementary metrics. The results showed that, in a similar way to other SAF production technologies, ATJ is not economically feasible, indicating that a process of technological maturity is necessary to reduce costs and economic incentives to improve its profitability. The main stage that limits and reduces the profitability of the process is the production of alcohols from biomass. This is due to the low yields of biomass to alcohol, which are around 15%, according to the data reported in Table S5 of the supplementary material. Additionally, this step requires significant amounts of energy to produce anhydrous alcohol. These low yields and high purification costs directly impact the sales costs and production of other co-products such as ethylene, diesel, or gasoline. In the case of the solution with the highest environmental impact and the highest net profit (see Pareto front Netprofit vs EI99), this solution corresponds to a situation where 15% of Mexico's biojet-fuel demand is satisfied, while the dot on the lower left side indicates a solution for which only 5.5% of the national demand was satisfied. It is important to emphasize this value of 15%, as it represents the maximum amount of biojet fuel that can be substituted using only corn stover and sugarcane bagasse as raw materials. The shape of the Pareto front for net profit vs. EI99 indicates that as more biofuel is produced and the demand coverage increases, economic losses and environmental impact also rise. This is because attempting to cover more biojet fuel demand requires additional biomass transport to pretreatment centers and biorefineries, as well as increased energy and costs due to the need for additional processing stages. Moreover, installing more biorefineries and pretreatment centers increases both environmental impact and costs. This can be verified by analyzing the graph of jobs created vs. net profit (Fig. 5). In the case of jobs created, it depends on the level of investment expenditure according to the JEDI methodology. Therefore, the higher the expenditure, the greater the losses, but more jobs are generated. Consequently, the solution with the most losses corresponds to the solution with the highest job creation. This is further reinforced by analyzing the graph of Net Profit vs. CO_2 emissions. The solution with the most losses is the solution with the highest CO_2 emissions. Finally, analyzing the Pareto front of Net Profit vs. Social Welfare, it can be noted that greater monetary loss (expenses) results in a better social welfare value, meaning that more airports receive biojet fuel, leading to a more equitable distribution of resources. These results are interesting because they indicate that achieving sustainable development goals such as Goal 8 (affordable and clean energy), Goal 12 (responsible consumption and

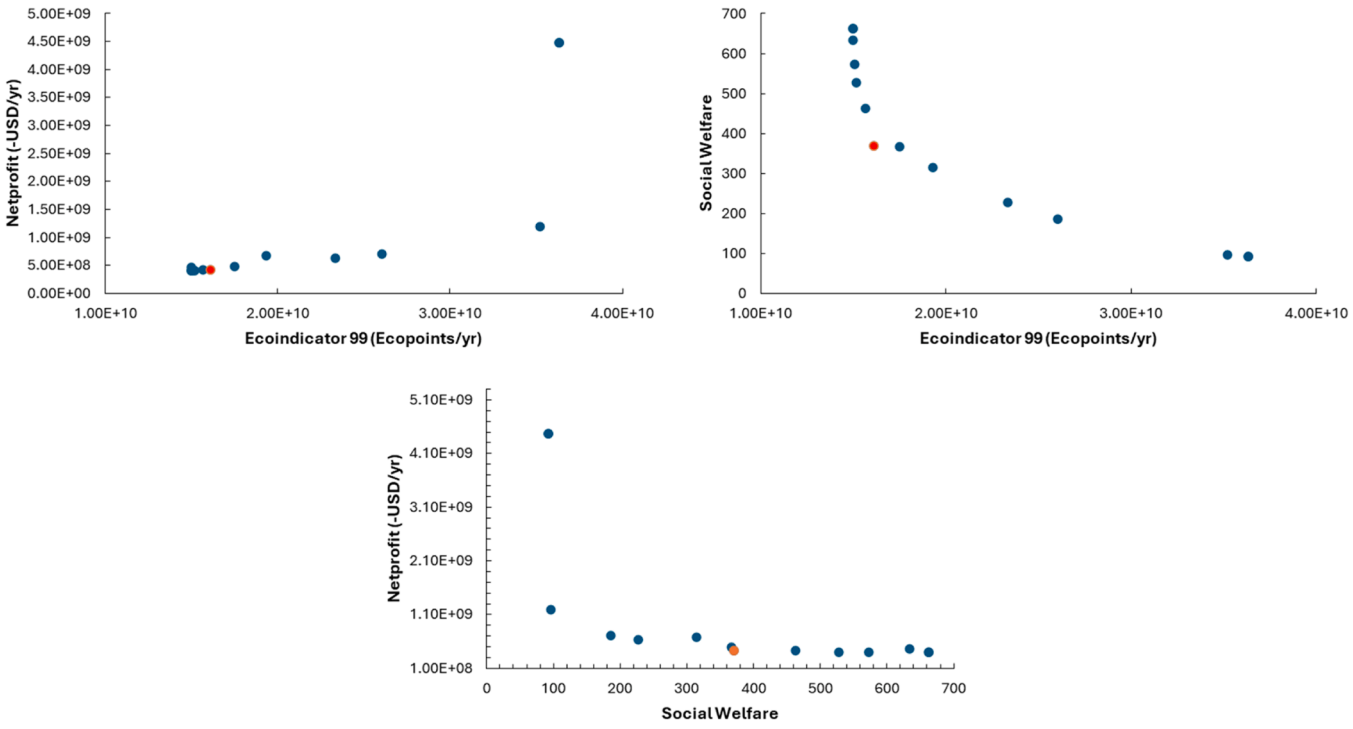

Fig. 4. Pareto fronts for the objective functions

Table 2
Indicator values for the optimal supply chain.

Indicator	Value
Net-profit (-USD/yr)	485,617,858.40
Eco-Indicator 99 (points/yr)	17,502,704,201.99
Social Welfare	367.19
Jobs Generated (Jobs/yr)	15,418
CO_2 emissions (kg CO_2 /kg Products)	2.2028

production), and Goal 13 (climate action) requires greater innovation in processing technologies. According to our results, substituting more fossil fuel with biojet fuel ironically leads to more pollution due to the factors previously mentioned. It is important to note that sales data for products like ethanol or ethylene are not included. This is because the model's optimization determined that including these sales is not necessary.

Based on the aforementioned, higher production levels lead to an escalation in transportation costs and require the establishment of additional biorefineries and pretreatment facilities. This drastically increases the environmental impact, cost, and complexity of the biomass supply chain, as more lignocellulosic waste is required and must be distributed to an increasing number of plants. Additionally, it can be observed that the Pareto fronts ha an asymptotic shape for smaller net profit and Eco indicator values. The reason is that the optimization was constrained to satisfy at least 5.5% of the demand in Mexico. Given these findings, it is clear that subsidies may be necessary to make production via the ATJ route more economically viable.

Observe the red dot on the Pareto front; this point was considered as the optimal solution. For the selection of this point, the social welfare objective was taken as a basis, where the goal is to ensure that all airports can have access to this biojet fuel. At this point, it can be observed that both the environmental impact is close to its minimum, and the economic incentives that would need to be provided for this process are also at their minimum. It is important to mention that, at this point, the objective of replacing 5.5% of the jet fuel demand with biojet fuel, as established by the Mexican government, is achieved. It is crucial to highlight that this study was conducted in the context of infrastructure in Mexico, considering that the primary means of transport is by road and that fossil fuels are used for such transportation. Our results clearly reveal that the replacement of jet fuel with biojet fuel alone is not sufficient and, on the contrary, becomes detrimental to the environment as more biojet fuel is produced. Therefore, a true improvement in environmental impact requires the joint adoption of new, less polluting transportation technologies in Mexico.

Regarding the Pareto front EI99 vs. Social Welfare (Fig. 4), please note that this figure shows an inverse relationship. It is important to remember that in this context, social welfare is determined by a dimensionless number ranging from 0 to 1 for a single market. A score of 1 denotes no demand satisfaction, while 0 signifies full demand fulfillment for a specific market. In a situation where the sum of social welfare scores at 670, it was observed the lowest environmental impact. This scenario involves supplying biojet-fuel to a limited number of airports, satisfying a minimum of 5.5% of their demand of the total Mexicos demand. The implementation of this strategy results in a reduced environmental footprint as this solution implies less biofuel and product distribution, minimized shipping, and the construction of fewer processing and pretreatment plants. A solution of this type simplifies the supply chain, reduces the number of plants, but only satisfies the needs of the larger airports in the country, relegating the smaller ones.

In contrast, a scenario that seeks to amplify social benefits by supplying more airports with sustainable aviation fuel results in a greater environmental impact. This situation corresponds with a solution where every airport meets 15% of their demand for jet fuel. However, this solution requires the establishment of more facilities to produce jet fuel and other co-products, as well as the addition of more pretreatment depots. Consequently, transportation emissions escalate due to an increase in the distribution of products and raw materials. Indeed, as the processing capacity of the supply chain expands, the introduction of pretreatment depots presents itself as a viable solution to support this growth while mitigating environmental impact. This further underscores the role of pretreatment depots as an eco-friendly alternative in the supply chain, especially when handling significant quantities of biomass.

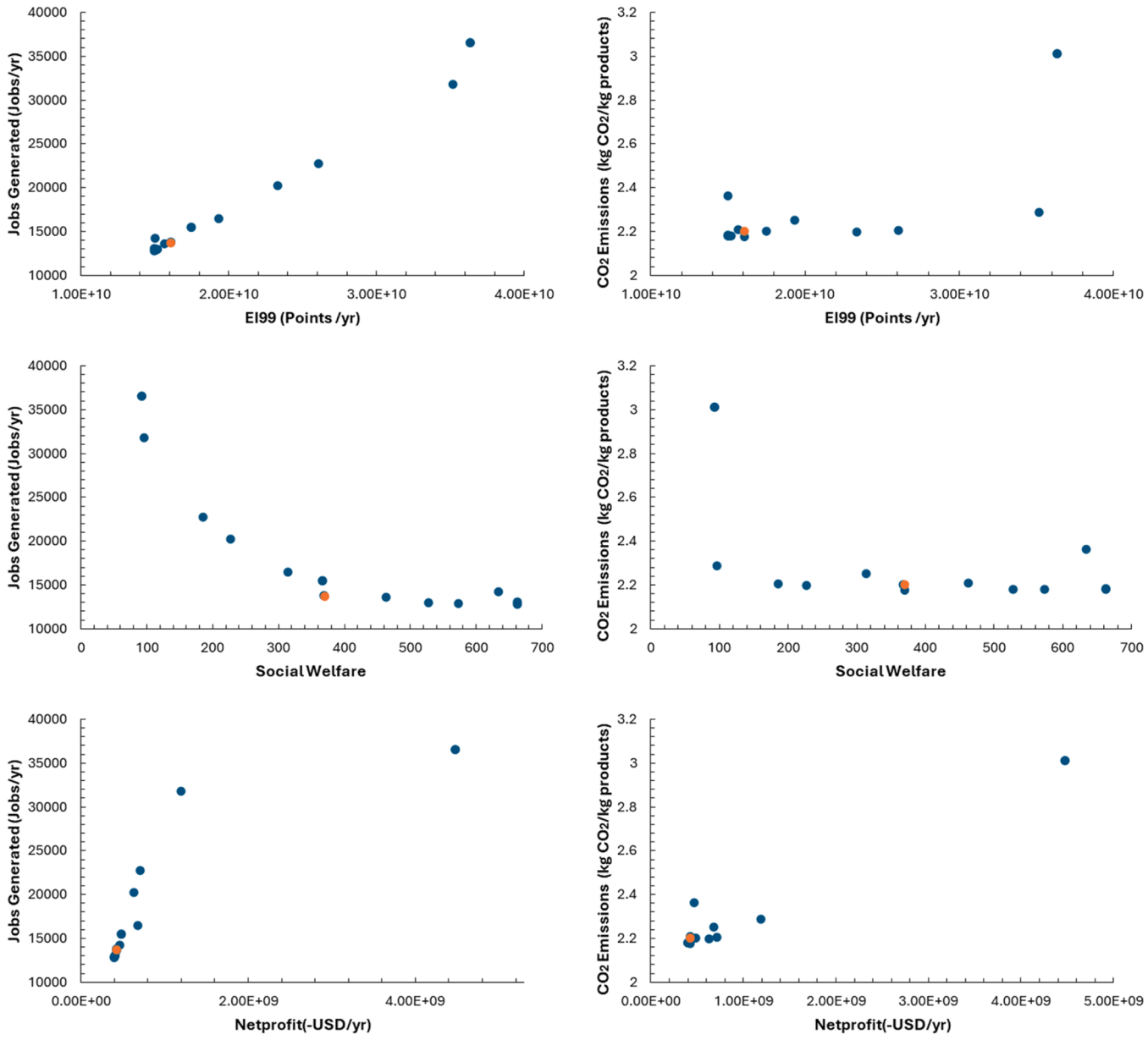

Fig. 5. Comparison of objective functions and complementary indexes

Furthermore, it is worth noting that the points on the Pareto front with values between 170 and 270 of social welfare considered the integration of pretreatment depots. This region of the Pareto front achieved a drastic decrease in social welfare without significantly compromising the environmental impact of the supply chain. Therefore, it can be said that the integration of pretreatment depots has a favorable effect in balancing both objectives, especially when the processing capacity of the supply chain increases considerably.

In the case of the eco-indicator concerning the complementary indices, which are job creation and CO2 emissions, it can be observed that increased job creation leads to higher environmental impacts. This is because implementing more plants and requiring more transportation routes benefits job creation but harms the environment by generating more emissions.

Finally, Fig. 4 also shows, the Pareto front between the social and economic, which reflects the opposing behavior between both objectives. However, it can be observed that as the distribution of jet-fuel decreases, the net gain of the supply chain only shows slight variations, indicating that meeting this demand does not significantly compromise the economic aspect, at least until this demand decreases drastically.

As can be seen for social welfare values between 100 and 300, net profit experiences a drastic increase. This is because, for these points, it is necessary to meet more demand at multiple airports, which significantly increases the number of installed plants. Consequently, production and raw material transportation costs are also drastically elevated. This increase in the installation of biorefineries and transportation results in a drastic increase in environmental impact, as observed in Pareto front environmental impact vs social welfare.

In the case of comparing social welfare with the complementary metrics, it can be observed that as the distribution of products becomes more equitable (lower welfare value), more jobs are created and CO2 emissions increase (see Fig. 5). This is because more plant installations and transportation routes are required

It is important to highlight that, the solution obtained by the mathematical model indicates the need for a hybrid production system, which is both modular and centralized. Centralized systems are required in states with abundant raw material availability, such as in the southern

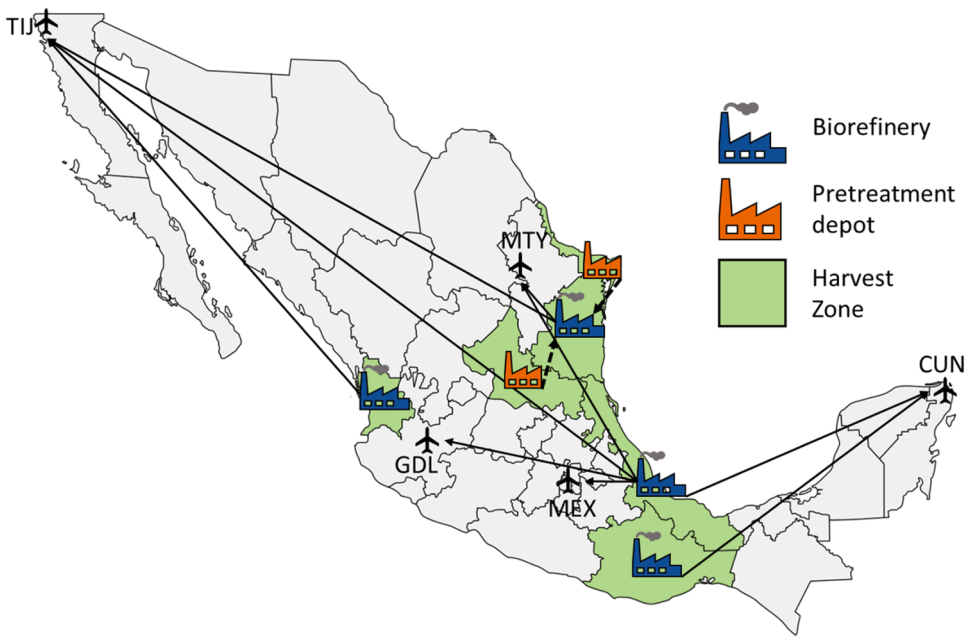

Fig. 6. Optimal supply chain for biojet-fuel.

states of Mexico, while in the northern and central states, a distributed system is preferred. In these distributed systems, biomass can be densified into ethanol and subsequently converted into biojet fuel. Considering the chosen optimal solution, it is deduced that it 6.3% of Mexico's total demand for SAF can be covered. This represents to approximately 330,898 m^3 of biojet-fuel. Fig. 6 displays the harvest centers, refineries, and pretreatment depots required to carry out the distribution of SAF for this solution. As depicted in Fig. 7, the proposed supply chain includes the establishment of four refineries and two pretreatment depots. These facilities collectively generate 32,482 m^3 of ethanol annually. It is important to highlight that this supply chain considers a decentralized approach, involving the use of pretreatment depots.

It is important to mention that the solution is only shown for the main airports in Mexico, which are: Mexico City (MEX), Cancun (CUN), Guadalajara (GDL), Monterrey (MTY), and Tijuana (TIJ). These airports were selected as representative solutions because they account for approximately 75% of jet fuel in Mexico.

Fig. 7 illustrates the required storage of biomass throughout the year for the selected point as the best solution. The results indicate that corn stover should be stored during January, February, and also in June and July. The storage in January and February primarily occurs in the southern states, where there is a higher availability of corn stover, allowing for its use later in seasons when availability is lower. It is important to highlight that in this region, the storage of corn stover is less, due to the greater abundance of bagasse. In the case of June and July, storage mainly occurs in the northern states of Mexico, to be able to use it in months when it is scarcer. Similarly, the storage of sugarcane bagasse primarily takes place in April and July to supply this raw material in periods when corn stover is scarce, which is typically in August and December in the northern states of Mexico.

According to this solution, this production of SAF requires an annual financial subsidy of $485 million to reach its breakeven point. As illustrated in Fig. 8a), the primary cost-drivers in this chain are the biomass pretreatment and hydrolysis (E1), ethanol fermentation and separation (E2), ethanol dehydration into ethylene (E3), and the conversion of ethylene to a paraffinic mixture through oligomerization, hydrogenation, and separation (E4). Notably, ethanol production forms a crucial part of the ATJ process, with the pretreatment and fermentation stages (E1 and E2) accounting for over half (53.67%) of the supply chain costs. This surpasses other areas such as transportation or fuel production and underscores the need of technological enhancements in these stages to achieve profitability.

The environmental impact of this supply chain, depicted in Fig. 8b),

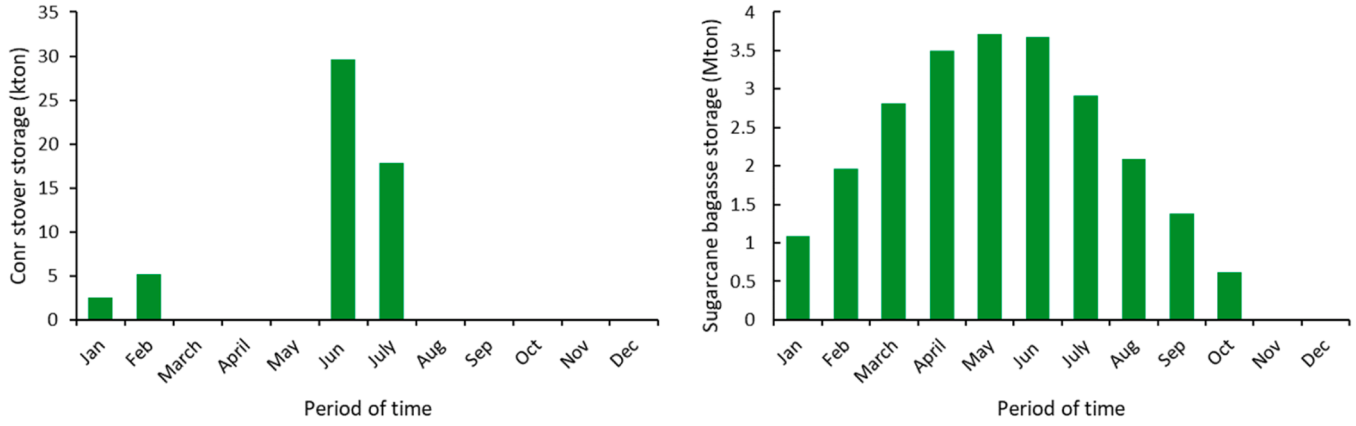

Fig. 7. Biomass inventory levels for a one-year time horizon.

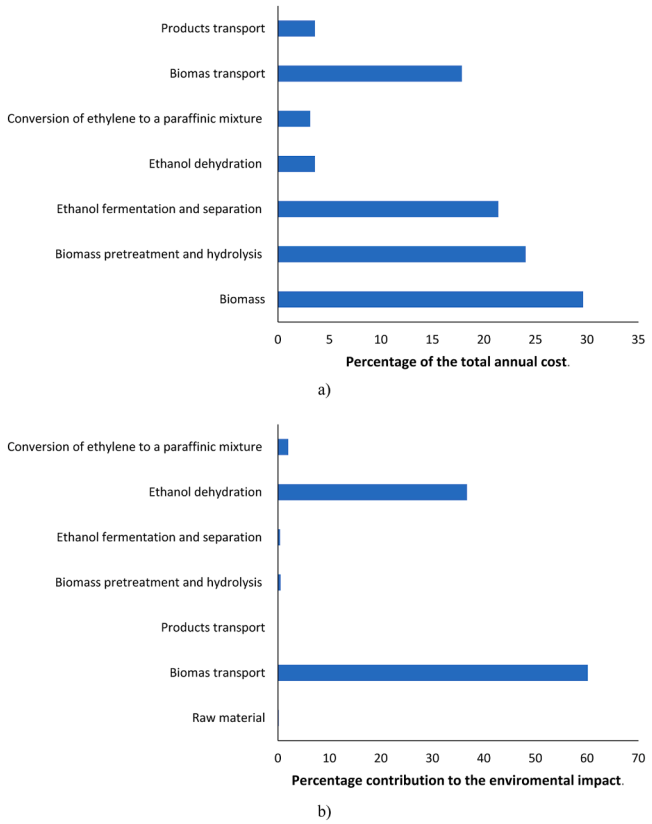

Fig. 8. a) Distribution of the cost for the supply chain b) Distribution of the environmental impact.

shows that the primary environmental burden stems from the dehydration stage. This phase demands substantial energy and is significantly influenced by the type of raw material used. Even though waste material forms the basis of the products, and itself does not contribute to the environmental burden, the collection process of such waste does. Given its wide geographical dispersion, the collection process requires substantial transportation and energy, thus contributing to the environmental impact. This finding underscores the necessity to devise efficient collection strategies for lignocellulosic waste that take its geographical spread into consideration.

Tabl3ble 5 illustrates the proportion of jet fuel demand that is satisfied at various airports. It reveals that the supply chain has the capacity to fulfill 50% of the jet fuel demand at 24 out of the 62 existing airports, which demonstrates its broad reach. However, the social welfare scheme, aimed at promoting wide stakeholder inclusion, particularly in areas of lower demand, appears to result in an uneven distribution of the biomass supply. The structure of the supply chain is predominantly centered around the central region of the country to meet the dimensionless jet fuel demand requirements. This region is selected due to its high concentration of airports, allowing for a reduction in environmental impact caused by the transportation of raw materials and final products. The setup further highlights the array of feasible solutions to manage similar social impacts as assessed through the social welfare scheme.

Fig. 9 complements this discussion by illustrating how the production configuration manages the fluctuating availability of biomass. It compares the biomass processed at harvesting centers with the total available biomass. As can be seen, even though the supply chain consumed only a fraction of the available biomass, the sustained biomass consumption by the supply chain did not exhibit the fluctuations observed in biomass availability. On the contrary, the management carried out by the supply chain surpassed the complete unavailability of

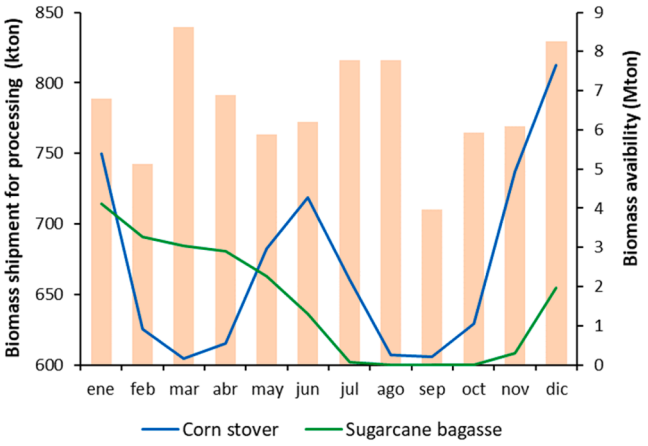

Fig. 9. Comparison between biomass availability and processing.

Table 3
Covered demand and supply of biojet fuel at airports in Mexico.

Airport Code	Demand satisfied (%)	(m^3/yr) of SAF supplied	Airport Code	Demand satisfied (%)	(m^3/yr) of SAF supplied
ACA	5.5	763.59	MZT	5.5	1,099.67
AGU	5.5	929.06	NLD	50	639.00
BJX	5.5	3,174.91	NOG	50	30.79
CEN	44.94	3,499.30	OAX	5.5	1,101.02
CJS	5.5	1,699.60	PAZ	50	409.79
CME	5.5	897.13	PBC	5.5	841.22
CLQ	50	1,617.21	PCA	50	229.93
CPE	50	2,421.38	PPE	50	76.23
CTM	50	3,838.35	PQM	50	231.28
CUL	5.5	2,197.76	PVR	5.5	5,808.04
CUN	5.5	40,199.273	PXM	50	2,504.85
CUU	5.5	1,813.63	QET	5.5	2,755.19
CVJ	50	402.61	REX	30.77	2,834.78
CVM	50	576.82	SJD	5.5	6,068.71
CZM	9.29	1,228.86	SLP	5.5	848.43
DGO	11.36	1,216.84	TAM	22.62	2,222.75
GDL	5.5	17,524.14	TAP	22.27	2,151.84
GYM	50	236.53	TCN	50	81.05
HMO	5.5	2,017.23	TGZ	5.5	1,301.35
HUX	5.5	988.39	TIJ	5.5	10,456.78
LAP	5.5	1,293.06	TLC	5.5	2,855.10
LMM	50	3,951.78	TSL	50	76.89
LTO	50	929.02	TPQ	50	1,835.57
LZC	50	366.40	TRC	5.5	764.77
MAM	50	858.96	UPN	50	2,238.04
MEX	5.5	85,718.53	VER	5.5	1,085.55
MID	5.5	3,250.37	VSA	5.5	1,261.91
MLM	5.5	1,356.73	ZCL	20.54	2,078.12
MTT	50	1,620.48	ZIH	17.78	1,948.75
MTY	5.5	10,640.25	ZLO	50	1,793.43
MXL	5.5	1,289.57	IZT	50	297.36

sugarcane bagasse observed between August and October, which represented a significant challenge to overcome, as the processing facilities operated in parallel for both biomass sources. Finally, Table 3 shows the percentage of biojet fuel covered. It can be seen that for all airports, a minimum of 5.5% of their demand is covered, and in some cases, up to 50% of the airport's demand is met, which confirms that it is feasible to replace 5.5% of jet fuel with biojet fuel in Mexico. Furthermore, this percentage could potentially be increased if other types of waste are considered.

10. Conclusions

In this study, a mathematical model was developed to determine the optimal production scheme for producing biojet fuel through the ATJ

process in Mexico. The model evaluates three operational schemes within the supply chain. Firstly, a typical centralize schemes where all the resources are sent to a single facility which produce all the products sent them to the different markets. The second operative scheme is a modular production in which different parts of the process are installed in different location in order to reduce operative an environmental cost. Finally, a hybrid operative scheme where coexists centralized a decentralized schemes is also considered. In addition, the model considers the production of ethanol and ethylene from the lignocellulosic residues of corn and sugarcane available in Mexican fields. The model was formulated as a mixed-integer linear problem to address issues such as seasonality and biomass localization, as well as the spatial distribution of markets, harvest centers, and potential locations for processing plants. The model considers net profit, environmental impact measured with the Eco-indicator 99, and social welfare as metrics to evaluate the performance of the solutions. Additionally, two complementary metrics, jobs created, and CO_2 emissions generated as a consequence of the production scheme, were evaluated. The model was formulated as a MILP model, and implemented in GAMS. The optimization of the supply chain prioritized sustainability, considering economic, environmental, and social aspects simultaneously, as these are the three fundamental pillars of sustainability. These objectives were tackled by maximizing net profit, minimizing EI99, and maximizing social welfare, which were harmonized using the constraint method.

The model was solved as a multi-objective optimization problem, using the e-constraint method. The selected solution aims to obtain a good trade-off between the Eco-Indicator 99, CO_2 emissions, as well as social objectives and metrics, which include job creation and social welfare. This solution consists of a net profit of -4.85 $\times$ 10^8 USD/yr, an Eco-Indicator 99 value of 1.7 $\times$ 10^9 ecopoints/yr, a social welfare value of 367.19, 15,488 jobs created per year, and CO2 emissions of 2.2 (kg CO2/kg Products). The optimal solution is capable of replacing up to 6.43% of the jet fuel. This solution employs a hybrid production system, in which 4 complete refineries and two pretreatment depots are placed in different locations.

The results show that it is feasible to cover up to 15% of the biojet fuel demand using only corn stover and sugarcane bagasse as raw materials, confirming that it is feasible to meet the goal of replacing 5.5% of jet fuel with biojet fuel. Additionally, the results show that it is possible to meet at least 5.5% of the airports' demand for biojet fuel, and in some cases, up to 50% of their demand.

Additionally, the results indicate that the social and environmental metrics display competitive behavior. Solutions with the least environmental impact and CO_2 emissions tend to be the worst in terms of job creation and equitable distribution of resources. This is because solutions with lower environmental impact require fewer plants and less transportation of raw materials and products. Primarily, it is considered that biorefineries and pretreatment depots operate using natural gas as the main energy source, and transport trucks use diesel as the main fuel. This is due to the current context in Mexico, where the use of renewable energies is limited. As future work, it is intended to modify the model to consider a technological mix in terms of energy sources and fuels, both renewable and non-renewable, and to vary the conversion efficiency at different stages of the ATJ process. The goal is to determine the mix of technological efficiency and use of fossil fuels that will allow meeting the Sustainable Development Goals of the 2030 Agenda. Finally, this work is a clear example of how a 4.0 process intensification approach can be a useful tool to find bottlenecks, in the more production schemes, which will help to meet the Sustainable Development Goals (SDGs).

CRediT authorship contribution statement

David Vallejo-Blancas: Writing – original draft, Validation, Methodology, Investigation, Formal analysis, Data curation. **Eduardo Sánchez-Ramirez:** Methodology, Data curation, Conceptualization. **José María Ponce-Ortega:** Validation, Supervision, Investigation, Formal analysis, Data curation, Conceptualization. **Juan Gabriel Segovia-Hernández:** Resources, Investigation, Conceptualization. **Juan José Quiroz Ramírez:** Writing – original draft, Supervision, Methodology, Formal analysis, Conceptualization. **Gabriel Contreras-Zarazúa:** Supervision, Methodology, Formal analysis, Conceptualization.

Declaration of competing interest

The authors declare that they have no known competing financial interests or personal relationships that could have appeared to influence the work reported in this paper.

Supplementary materials

Supplementary material associated with this article can be found, in the online version, at doi:10.1016/j.cep.2024.110078.

Data availability

Data will be made available on request.

References

[1] D. Tóthová, M. Heglasová, Measuring the environmental sustainability of 2030 Agenda implementation in EU countries: how do different assessment methods affect results? J. Environ. Manage. 322 (2022) https://doi.org/10.1016/j.jenvman.2022.116152.
[2] Transforming our world: the 2030 Agenda for Sustainable Development, Department of Economic and Social Affairs, 2015. |.
[3] I. Siksnelyte-Butkiene, Impact of the COVID-19 pandemic to the sustainability of the energy sector, Sustain 13 (2021), https://doi.org/10.3390/su132312973.
[4] Q. Wang, R. Huang, The impact of COVID-19 pandemic on sustainable development goals – a survey, Environ. Res. 202 (2021) 111637, https://doi.org/10.1016/j.envres.2021.111637.
[5] J.G. Segovia-Hernández, S. Hernández, E. Cossío-Vargas, E. Sánchez-Ramírez, Challenges and opportunities in process intensification to achieve the UN's 2030 agenda: Goals 6, 7, 9, 12 and 13, Chem. Eng. Process. - Process Intensif. 192 (2023), https://doi.org/10.1016/j.cep.2023.109507.
[6] A.I. Stankiewicz, J.A. Moulijn, Process intensification transforming chemical engineering, (2000) 22–34. https://www.aiche.org/sites/default/files/docs/news/010022_cep_stankiewicz.pdf.
[7] J. Bielenberg, M. Bryner, Realize the potential of process intensification, Chem. Eng. Prog. 114 (2018) 41–45.
[8] E.A. López-Guajardo, F. Delgado-Licona, A.J. Álvarez, K.D.P. Nigam, A. Montesinos-Castellanos, R. Morales-Menendez, Process intensification 4.0: A new approach for attaining new, sustainable and circular processes enabled by machine learning, Chem. Eng. Process. - Process Intensif. 180 (2022), https://doi.org/10.1016/j.cep.2021.108671.
[9] E. Villicaña-García, L.F. Lira-Barragán, J.M. Ponce-Ortega, Intensification 4.0 of hydraulic fracturing process involving incentive schemes and the use of matching law, Chem. Eng. Process. - Process Intensif. 176 (2022), https://doi.org/10.1016/j.cep.2022.108968.
[10] D.C. Boffito, D.Fernandez Rivas, Process intensification connects scales and disciplines towards sustainability, Can. J. Chem. Eng. 98 (2020) 2489–2506, https://doi.org/10.1002/cjce.23871.
[11] A. Bhosekar, M. Ierapetritou, Modular design optimization using machine learning-based flexibility analysis, J. Process Control. 90 (2020) 18–34, https://doi.org/10.1016/j.jprocont.2020.03.014.
[12] I.R.E.A. (IRENA), Reaching zero with renewables biojet fuels, 2021. https://www.irena.org/-/media/Files/IRENA/Agency/Publication/2021/Jul/IRENA_Reaching_Zero_Biojet_Fuels_2021.pdf.
[13] International Air Transport Association (IATA), Air passenger numbers to recover in 2024, (2022). https://www.iata.org/en/pressroom/2022-releases/2022-03-01-01/(accessed August 1, 2022).
[14] ASTM, Standard specification for aviation turbine fuel containing synthesized hydrocarbons, Annu. B. ASTM Stand. 7 (2017) 1–16, https://doi.org/10.1520/D7566-21.operated.
[15] S. Geleynse, K. Brandt, M. Garcia-Perez, M. Wolcott, X. Zhang, The alcohol-to-jet conversion pathway for drop-in biofuels: techno-economic evaluation, ChemSusChem. 11 (2018) 3728–3741, https://doi.org/10.1002/cssc.201801690.
[16] Rivas-Interian, Eduardo Sanchez-Ramirez, J.J. Quiroz-Ramírez, J.G. Segovia-Hernandez, Feedstock planning and optimization of a sustainable distributed configuration biorefinery for biojet fuel production via ATJ process, Biofuels, Bioprod. Biorefining. (2022).
[17] A.G. Romero-Izquierdo, F.I. Gómez-Castro, C. Gutiérrez-Antonio, S. Hernández, M. Errico, Intensification of the alcohol-to-jet process to produce renewable aviation fuel, Chem. Eng. Process. - Process Intensif. 160 (2021) 1–11, https://doi.org/10.1016/j.cep.2020.108270.

[18] G. Contreras-Zarazúa, E. Sánchez-Ramirez, E.A. Hernández-Vargas, J.G. Segovia-Hernández, J.J.Q. Ramírez, Process intensification in bio-jet fuel production: Design and control of a catalytic reactive distillation column for oligomerization, Chem. Eng. Process. - Process Intensif. 193 (2023), https://doi.org/10.1016/j.cep.2023.109548.
[19] B. Huerta-Rosas, E. Sánchez-Ramírez, G. Contreras-Zarazua, J.J. Quíroz-Ramírez, O.A. Luevano-Rivas, J.G. Segovia-Hernández, Design and optimization of an intensified sustainable plant to produce biojet fuel using the ATJ process, Chem. Eng. Process. - Process Intensif. 200 (2024), https://doi.org/10.1016/j.cep.2024.109774.
[20] Z. Said, T.H. Nguyen, P. Sharma, C. Li, H.M. Ali, V.N. Nguyen, V.V. Pham, S. F. Ahmed, D.N. Van, T.H. Truong, Multi-attribute optimization of sustainable aviation fuel production-process from microalgae source, Fuel 324 (2022) 124759, https://doi.org/10.1016/j.fuel.2022.124759.
[21] Ministry of Agriculture and Fishing, SAGARPA, 2019. http://infosiap.siap.gob.mx/gobmx/datosAbiertos.php.
[22] E.S.R. Escalante, L.S. Ramos, C.J. Rodriguez Coronado, J.A. de Carvalho Júnior, Evaluation of the potential feedstock for biojet fuel production: focus in the Brazilian context, Renew. Sustain. Energy Rev. 153 (2022), https://doi.org/10.1016/j.rser.2021.111716.
[23] G. Contreras-Zarazúa, M. Martin, J.M. Ponce-Ortega, J.G. Segovia-Hernández, Sustainable design of an optimal supply chain for furfural production from agricultural wastes, Ind. Eng. Chem. Res. 60 (2021) 14495–14510, https://doi.org/10.1021/acs.iecr.1c01847.
[24] J. Harmsen, J.B. Powell, Sustainable development in the process industries: cases and impact, 2010. https://doi.org/10.1002/9780470586099.
[25] S. de energía de M. (SENER), Prospectiva de energías renovables 2016-2030, 2016. https://www.gob.mx/cms/uploads/attachment/file/177622/Prospectiva_de_Energ_as_Renovables_2016-2030.pdf.
[26] S. de comunicaciones y transportes (SCT), Plan de acción para mitigar las emisiones de gases de efecto invernadero de la aviación civil Mexicana, 2016. https://www.gob.mx/cms/uploads/attachment/file/578886/PA_2015-2018_1.pdf.
[27] ASTM, Evaluation of new aviation turbine fuels and fuel additives, (2021). https://doi.org/10.1177/089033449801400218.
[28] R.T.L. Ng, C.T. Maravelias, Design of biofuel supply chains with variable regional depot and biorefinery locations, Renew. Energy. 100 (2017) 90–102, https://doi.org/10.1016/j.renene.2016.05.009.
[29] R.T.L. Ng, C.T. Maravelias, Design of cellulosic ethanol supply chains with regional depots, Ind. Eng. Chem. Res. 55 (2016) 3420–3432, https://doi.org/10.1021/acs.iecr.5b03677.
[30] C. Hernández, C. Escamilla-Alvarado, A. Sánchez, E. Alarcón, F. Ziarelli, R. Musule, I. Valdez-Vazquez, Wheat straw, corn stover, sugarcane, and Agave biomasses: chemical properties, availability, and cellulosic-bioethanol production potential in Mexico, Biofuels, Bioprod. Biorefining. 13 (2019) 1143–1159, https://doi.org/10.1002/bbb.2017.
[31] B. Purvis, Y. Mao, D. Robinson, Three pillars of sustainability: in search of conceptual origins, Sustain. Sci. 14 (2019) 681–695, https://doi.org/10.1007/s11625-018-0627-5.
[32] S. Potrč, L. Čuček, M. Martin, Z. Kravanja, Synthesis of european union biorefinery supply networks considering sustainability objectives, Processes 8 (2020) 1–25, https://doi.org/10.3390/pr8121588.
[33] M. Goedkoop, R. Spriensma, The eco-indicator 99 - a damage oriented method for life cycle impact assessment, Assessment. 144 (2001).
[34] U.S.G. Council, Ethanol, fuels and co-product pricing, 2021. https://grains.org/ethanol_report/ethanol-market-and-pricing-data-october-1-2019/.
[35] OPIS PetroChemWire, Petrochem Wire Daily, Today in the market, 2020. https://info.opisnet.com/hubfs/PCWDaily-Sample062819.pdf?hsLang=en.
[36] C.R. de E. (CRE), Precios máximos de venta de primera mano y terminales de almacenamiento de petrolífero, n.d. https://datos.gob.mx/busca/dataset/precios-maximos-de-venta-de-primera-mano-y-terminales-de-almacenamiento-de-petroliferos.
[37] T. Pinto-Varela, A.P.F.D. Barbosa-Póvoa, A.Q. Novais, Bi-objective optimization approach to the design and planning of supply chains: economic versus environmental performances, Comput. Chem. Eng. 35 (2011) 1454–1468, https://doi.org/10.1016/j.compchemeng.2011.03.009.
[38] A. Hugo, E.N. Pistikopoulos, Environmentally conscious long-range planning and design of supply chain networks, J. Clean. Prod. 13 (2005) 1471–1491, https://doi.org/10.1016/j.jclepro.2005.04.011.
[39] M.S. Pishvaee, J. Razmi, Environmental supply chain network design using multi-objective fuzzy mathematical programming, Appl. Math. Model. 36 (2012) 3433–3446, https://doi.org/10.1016/j.apm.2011.10.007.
[40] D. Russo, G. Bersano, V. Birolini, R. Uhl, European testing of the efficiency of TRIZ in eco-innovation projects for manufacturing SMEs, Procedia Eng. 9 (2011) 157–171, https://doi.org/10.1016/j.proeng.2011.03.109.
[41] J.E. Santibañez-Aguilar, J.B. González-Campos, J.M. Ponce-Ortega, M. Serna-González, M.M. El-Halwagi, Optimal planning and site selection for distributed multiproduct biorefineries involving economic, environmental and social objectives, J. Clean. Prod. 65 (2014) 270–294, https://doi.org/10.1016/j.jclepro.2013.08.004.
[42] A. del C. Munguía-López, A.M. Sampat, E. Rubio-Castro, J.M. Ponce-Ortega, V. M. Zavala, Fairness-guided design of water distribution networks for agricultural lands, Comput. Chem. Eng. 130 (2019), https://doi.org/10.1016/j.compchemeng.2019.106547.
[43] G. Mavrotas, Effective implementation of the ε-constraint method in Multi-Objective Mathematical Programming problems, Appl. Math. Comput. 213 (2009) 455–465, https://doi.org/10.1016/j.amc.2009.03.037.
[44] J. Ren, D. An, H. Liang, L. Dong, Z. Gao, Y. Geng, Q. Zhu, S. Song, W. Zhao, Life cycle energy and CO2 emission optimization for biofuel supply chain planning under uncertainties, Energy 103 (2016) 151–166, https://doi.org/10.1016/j.energy.2016.02.151.
[45] L.C. Nhien, N.V.D. Long, S. Kim, M. Lee, Design and optimization of intensified biorefinery process for furfural production through a systematic procedure, Biochem. Eng. J. 116 (2016) 166–175, https://doi.org/10.1016/j.bej.2016.04.002.
[46] T. Palander, The environmental emission efficiency of larger and heavier vehicles – a case study of road transportation in Finnish forest industry, J. Clean. Prod. 155 (2017) 57–62, https://doi.org/10.1016/j.jclepro.2016.09.095.
[47] M.D. Shields, J. Zhang, The generalization of Latin hypercube sampling, Reliab. Eng. Syst. Saf. 148 (2016) 96–108, https://doi.org/10.1016/j.ress.2015.12.002.
[48] Ministry of rural development, SADER, 2019.